

**DESIGN, FABRICATION AND CHARACTERIZATION OF A DOUBLE-NETWORK  
ALGINATE-PHEMA HYDROGEL COATING FOR PDMS-BASED BIOMEDICAL  
IMPLANTS**

by

Zhengmu Wang

B.Sc., B.M.E., University of Minnesota, 2014

A THESIS SUBMITTED IN PARTIAL FULFILLMENT OF  
THE REQUIREMENTS FOR THE DEGREE OF

MASTER OF APPLIED SCIENCE

in

THE FACULTY OF GRADUATE AND POSTDOCTORAL STUDIES  
(Mechanical Engineering)

THE UNIVERSITY OF BRITISH COLUMBIA  
(Vancouver)

March 2017

© Zhengmu Wang, 2017

## Abstract

Traditional silicone biomedical implants, such as urinary catheters, often suffer from high surface friction, high stiffness, and a lack of hydrophilicity, which can cause discomfort or discomfort. To tackle these challenges, we developed a double-network alginate-pHEMA hydrogel “cushion” coating for polydimethylsiloxane (PDMS) biomedical implants. The double-network hydrogel presented here consists of two distinct networks made of alginate and pHEMA, respectively. The alginate network is covalently bonded to PDMS substrates as scaffolding, and the denser pHEMA network fills the free space within the alginate network. In this proof of concept study, the double-network hydrogel achieved a compressive fracture stress of  $502.04 \pm 14.41$  kPa, which is 5.8-fold stronger than the alginate hydrogel, while its elasticity is still comparable to soft tissues. The proposed double-network hydrogel has a negligible amount of swelling in biological fluids and exhibits no cytotoxicity, which are desirable qualities for biomedical and coating applications. Both chemical modification using APTES and micropillar anchors have been used to improve the coating stability. We found that the adhesion strength of the hydrogel coating on micropillar PDMS substrates is 55% stronger than on bare PDMS substrates when both substrates are grafted with APTES. In comparison to native PDMS and K-Y Jelly-lubricated PDMS, the double-network alginate-pHEMA hydrogel-coated PDMS demonstrated significantly less friction and superior hydrophilicity.

## **Preface**

The research presented in this thesis was carried out at the University of British Columbia and its affiliated facilities under the supervision of Dr. Mu Chiao of the Mechanical Engineering Department. Except for the cytotoxicity study (Chapter 2), all aspects of the work, including literature review, design and fabrication of proposed materials, characterization, analysis, and discussion of the research data was performed solely by the author of this thesis. The experimental part of the cytotoxicity study was conducted in collaboration with Axel Chu of the Department of Mechanical Engineering and Dr. Chinten James Lim of the Department of Pediatrics. The samples for the cytotoxicity study were prepared by the author of this thesis, while the *in vitro* experiments were conducted by Axel Chu. The data acquired from the cytotoxicity study was analyzed solely by the author of this thesis.

# Table of Contents

<b>Abstract.....</b>	<b>ii</b>
<b>Preface.....</b>	<b>iii</b>
<b>Table of Contents .....</b>	<b>iv</b>
<b>List of Tables .....</b>	<b>vii</b>
<b>List of Figures.....</b>	<b>viii</b>
<b>List of Symbols and Abbreviations .....</b>	<b>x</b>
<b>Acknowledgements .....</b>	<b>xiv</b>
<b>Chapter 1: Introduction .....</b>	<b>1</b>
1.1    PDMS-based Biomedical Implants.....	1
1.2    Surface Modifications for PDMS-based Implants .....	2
1.2.1    Energy Treatments .....	3
1.2.2    Teflon Coating .....	4
1.2.3    Hydrogel Coatings .....	5
1.2.3.1    Radiation-induced Graft Method .....	5
1.2.3.2    Chemical Tailoring Method .....	5
1.3    Types of Hydrogels.....	6
1.3.1    PVA Hydrogel .....	7
1.3.2    PEG Hydrogel.....	7
1.3.3    PHEMA Hydrogel .....	7
1.3.4    Alginate Hydrogel.....	8
1.3.5    DN Hydrogels .....	8

1.4	DN Alginate-pHEMA Hydrogel Coating .....	10
1.5	Thesis Overview .....	11
<b>Chapter 2: Double-Network (DN) Alginate-pHEMA Hydrogel.....</b>		<b>13</b>
2.1	Polymerization Mechanism .....	13
2.1.1	Alginate Network.....	13
2.1.2	PHEMA Network.....	15
2.2	Hydrogel Preparation .....	16
2.2.1	Single-Network (SN) Alginate Hydrogel .....	16
2.2.2	Double-Network (DN) Alginate-pHEMA Hydrogel .....	17
2.3	Characterizations.....	18
2.3.1	Analysis of Mechanical Properties .....	18
2.3.2	Swelling Coefficient and Water Content Comparison.....	19
2.3.3	Cytotoxicity Study .....	20
2.4	Results and Discussion .....	21
2.4.1	Mechanical Properties.....	21
2.4.2	Microstructure.....	29
2.4.3	Swelling Coefficient and Water Content .....	32
2.4.4	Cytotoxicity Study .....	34
<b>Chapter 3: DN Hydrogel Coating for PDMS Devices .....</b>		<b>36</b>
3.1	Fabrication Process .....	36
3.1.1	Fabrication of PDMS Micropillar Substrates .....	36
3.1.2	Surface Modification of PDMS Micropillar Substrates.....	37
3.1.3	SN Alginate Hydrogel Coating Formation .....	38

3.1.4	DN Alginate-pHEMA Hydrogel Coating Formation .....	39
3.2	Characterizations.....	41
3.2.1	Detecting APTES.....	41
3.2.2	Friction Coefficient Measurement .....	41
3.2.3	Contact Angle Measurement.....	43
3.2.4	Evaluation of Hydrogel-PDMS Bonding Strength .....	43
3.3	Results and Discussion .....	45
3.3.1	Chemical Modification on PDMS Substrates .....	45
3.3.2	Adhesion Strength between Coating and Substrate .....	47
3.3.3	Wettability and Friction Coefficient of Gel-coated Surface .....	49
<b>Chapter 4:</b>	<b>Conclusion .....</b>	<b>52</b>
4.1	Summary.....	52
4.2	Future Work.....	54
<b>References .....</b>		<b>56</b>
<b>Appendices.....</b>		<b>65</b>
Appendix A :	Fabrication Process of PDMS-Coated Glass Coverslip .....	65
Appendix B :	Double-Network Alginate-pHEMA Hydrogel Synthesis.....	66
Appendix C :	ImageJ Operation Guide.....	67
Appendix D :	Fabrication procedures for Micropillar Substrate Cast .....	68
Appendix E :	Ribbon Design for Hydrogel Adhesion Strength Test.....	69

## List of Tables

Table 1.1 Summarized implant surface modification methods. ....	2
Table 1.2 A list of hydrogels for biomedical applications .....	6

## List of Figures

Figure 1.1 Oxygen plasma treatment for PDMS surface. ....	3
Figure 1.2 SN alginate gel (left) and DN alginate-pHEMA gel (right). ....	10
Figure 2.1 Schematics of the two networks of alginate-polyHEMA hydrogel; (a) alginate network, (b) diffusion of HEMA monomers, (c) resulting DN structure, (d) alginate chains covalently crosslinked by AAD (purple circles), (e) HEMA monomers covalently crosslinked by MBAA (green triangles). ....	14
Figure 2.2 Fabrication setup for SN alginate hydrogel dishes. ....	16
Figure 2.3 Setup for hydrogel slicing experiment. ....	19
Figure 2.4 (a) Stress-strain curves and (b) Young's modulus. ....	23
Figure 2.5 (a) Fracture stress and (b) fracture strain. ....	24
Figure 2.6 (a) Stress-strain curves and (b) Young's modulus. ....	26
Figure 2.7 (a) Fracture stress and (b) fracture strain. ....	27
Figure 2.8 Slicing resistance of (a) SN alginate gel and (b) DN alginate-pHEMA gel. ....	28
Figure 2.9 (a) SN alginate hydrogel and (b) DN alginate-pHEMA hydrogel; (1) 50× magnification on the surface, (2) 50× magnification on the cross-section, (3) 250× magnification on the cross-section, and (4) 1500× magnification on the cross-section. ....	31
Figure 2.10 (a) Swelling coefficient and (b) equilibrium water content. ....	33
Figure 2.11 (a) OM images and (b) percentage confluence of HEK cells incubated with SN, DN gel and in control. ....	35

Figure 3.1 (a) Illustration of the CAD model of 20 mm × 20 mm substrate master; (b) The plastic master printed by Asiga Pico printer; (c) SEM image of micropillar substrate; and (d) close-up of a single micropillar. ....	37
Figure 3.2 Chemical modification on PDMS substrate and DN hydrogel coating formation. ....	38
Figure 3.3 DN hydrogel coating procedures. ....	39
Figure 3.4 SEM and OM images of the cross-sections of DN gel coating on micropillar substrates. ....	40
Figure 3.5 (a) The schematic and dimensions of the printed plastic mold for PDMS test pin (unit: mm) and (b) a printed plastic mold and cured PDMS test pin cast from the mold. ....	42
Figure 3.6 (a) Fabrication process for the lap-shear test strips, (b) the cross-section view of test ribbon with micropillars, (c) the cross-section view of test ribbon without micropillars, and (d) experiment setup. ....	44
Figure 3.7 FT-IR spectroscopy of bare PDMS, OH-PDMS and APTES-PDMS. ....	46
Figure 3.8 (a) Maximal force to separate the bonded strips, (b) separated micropillar strips and (c) separated bare PDMS strips. ....	48
Figure 3.9 Water droplets on (a) bare PDMS, (b) lubricated PDMS and (c) DN hydrogel surface, and (d) the contact angles of water on these surfaces. ....	50
Figure 3.10 (a) Friction coefficient of various substrates and (b) their comparison. ....	51
Figure A.1 The schematics of the master. ....	69

## List of Symbols and Abbreviations

°	degree of angle
°C	Celsius degree
%	percentage
3D	three dimensional
μl	microliter
μm	micrometer
AAD	adipic acid dihydrazide
AMPS	2-acrylamido-2-methylpropane sulfonic acid
APTES	(3-aminopropyl) triethoxysilane
Ca <sup>2+</sup>	calcium ion
CaCl <sub>2</sub>	calcium chloride
CaCO <sub>3</sub>	calcium carbonate
CaSO <sub>4</sub>	calcium sulfate
CBMAX	carboxybetaine crosslinker
cm <sup>-1</sup>	per centimeter
CO <sub>2</sub>	carbon dioxide
DMEM/F-12	Dulbecco's modified eagle medium: nutrient mixture F-12
DN	double-network
EDC	1-ethyl-3-(3-dimethylaminopropyl) carbodiimide
FT-IR	Fourier transform infrared spectroscopy

GDL	glucono- $\delta$ -lactone
h	hour
HCl	hydrochloric acid
HEK	human embryonic kidney
HEMA	2-hydroxyethyl methacrylate
H <sub>2</sub> O <sub>2</sub>	hydrogen peroxide
in	inch
kPa	kilopascal
m	mass
MES	2-(N-morpholino) ethanesulfonic acid
MBAA	N,N'-Methylene bisacrylamide
Mg <sup>2+</sup>	magnesium ion
min	minute
mm	millimeter
mM	milli-mol
mTorr	milli-torr
N	newton
nm	nanometer
Na <sup>+</sup>	sodium ion
NaOH	sodium hydroxide
NHS	N-Hydroxysuccinimide
O <sub>2</sub>	oxygen

OM	optical microscope
PAAm	poly(acrylamide)
PBS	phosphate-buffered saline
PDMS	polydimethylsiloxane
PEG	polyethylene glycol
pH	acidity scale
pHEMA	poly(2-hydroxyethyl methacrylate)
PTFE	polytetrafluoroethylene/Teflon
PVA	polyvinyl alcohol
RPM	revolutions per minute
s	second
S.C.	swelling coefficient
SEM	scanning electron microscope
Si	silicon
SN	single-network
TFEA	2,2,2-trifluoroethyl acrylate
TMSPMA	3-(trimethoxysilyl)propyl methacrylate
UTI	urinary tract infection
UV	ultraviolet
vol-%	volume to volume percentage
W	watt
W.C.	water content

wt-%

weight to weight percentage

mol-%

molar mass to molar mass percentage

## **Acknowledgements**

First and foremost, I would like to offer my enduring gratitude to my supervisor, Dr. Mu Chiao, who has given me this valuable opportunity to work in the MEMS lab that funded this project. I am grateful for his continuous support and guidance. I would also like to express my sincerest appreciation to my colleague and mentor Dr. Hongbin Zhang, for the training and insightful advice on the material science aspects of my project. My gratitude also goes to my colleague Axel Chu, for his expertise and work on the cytotoxicity study part of this project. Last but not least, I owe thanks to Dr. Helen Burt and John Jackson from the Department of Pharmaceutical Science, Dr. Hongshen Ma from the Department of Mechanical Engineering, and Dr. Karen Cheung from the Department of Electrical Engineering for allowing me to use their labs and equipment.

My lab mates Guangyi Cao, Aurora Chen, Keqin Chen, Ali Shademani, Kaiwen Yuan, Payam Zachkani, and Yibo Zhang of the MEMS lab have been supportive and helped to get me up to speed with my courses and experiments.

Special thanks are owed to my parents, who financially supported me throughout my years of education.

# **Chapter 1: Introduction**

## **1.1 PDMS-based Biomedical Implants**

Polydimethylsiloxane (PDMS) has been one of the most widely-used silicone-based organic elastomers in the manufacturing of biomedical devices, such as facial prosthetics, implants and contact lenses, because of its biocompatibility, optical transparency, ease of fabrication, gas permeability, and chemical inertness [1-4]. In recent years, it has become increasingly popular in microfluidics devices, drug delivery reservoirs and tissue engineering with the emergence of BioMEMS and new microfabrication techniques [5-7]. Despite the tremendous merits of PDMS, its usage is limited by its extreme hydrophobic nature that can easily cause surface contamination and hinder the introduction of aqueous solutions [8].

Although it is commonly used for implants like catheters, the PDMS surface tends to absorb undesired biomolecules that can attract bacteria and form a layer of biofilm, ultimately causing urinary tract infection (UTI) [9-11]. Catheter-induced UTI is considered the most common nosocomial infection, and catheters must be frequently changed to avoid this problem. Not only does it increase healthcare costs, but it also causes patients great discomfort during insertion and removal of catheters [12-14]. Furthermore, the high friction surface of PDMS-based catheters may cause intolerable pain to patients, or in rare cases, damage the mucous membranes of inserted organs if lubrication is not properly applied [15]. Surgical lube or lidocaine jelly is commonly used to lower the surface friction and local anesthetic may be used to reduce the discomfort during catheterization, though mixed results have been reported, questioning the effectiveness of such

methods [14, 16]. In addition, lubrications may become useless after being eluted by body fluids, making the removal of these implants even more challenging.

## 1.2 Surface Modifications for PDMS-based Implants

To tackle the above-mentioned issues, numerous surface modification methods have been introduced to improve the hydrophilicity and/or reduce the friction of implant surfaces [8, 17-20]. These methods can be roughly classified into three categories: energy treatments, Teflon coating and hydrogel coatings. The energy treatment methods rely on plasma or UV radiation to couple new molecular groups (usually hydrophilic) onto device surfaces; the latter two methods use a thin layer of polymer that isolates the implants from the adjacent environment [8]. A few notable surface modification methods are introduced in the following sections and summarized in Table 1.1.

Types of Modification	Function	Notes
Energy Treatments	Temporarily reduce hydrophobicity	Two common methods: oxygen plasma and ozone/UV treatments [17, 18] Last hours to days due to hydrophobic recovery [21, 22]
Teflon Coating	Low friction, improve comfort	Ultra-low frictional, extremely hydrophobic [19] Stiff; cracking induces toxicity [23, 24]
Hydrogel Coatings	Reduce friction, increase hydrophilicity	Radiation-induced graft method: UV induced radicals link to monomers with double bonds [8] Chemical tailoring method: reagents coated on implant surface covalently crosslink with hydrogel monomers [25, 26]

**Table 1.1 Summarized implant surface modification methods.**

### 1.2.1 Energy Treatments

Oxygen plasma treatment is one of the most common methods for PDMS surface modification today (Figure 1.1). The method uses partially ionized particles to bombard and oxidize the PDMS surface, creating chemical functional groups [17]. After the surface is treated with oxygen plasma, hydroxyl groups are coupled to Si atoms of the PDMS. Mata et al. [27] demonstrated that the hydrophilic hydroxyl groups can dramatically improve the hydrophilicity of a PDMS surface, reducing water contact angle from  $109^\circ$  to  $60^\circ$ . Nevertheless, a major challenge with the plasma oxidation treatment of PDMS is the hydrophobic recovery caused by chains scission and reorientation of hydroxyl groups from the surface into the bulk [28]. The original hydrophobicity is regained within a few hours to a few days [21]. The solvent extraction method proposed by Vickers et al. [29] can overcome this problem and produce more of a hydrophilic surface with a significant lower hydrophobic recovery rate. Alternatively, Ren et al. [22] indicated that the hydrophilicity of PDMS can be preserved for more than 14 days if the surface is in contact with water.

A PDMS surface can also be oxidized by UV/ozone treatment. Although this method is slower in terms of time, the penetration depth is greater than that of the oxygen plasma treatment, creating a

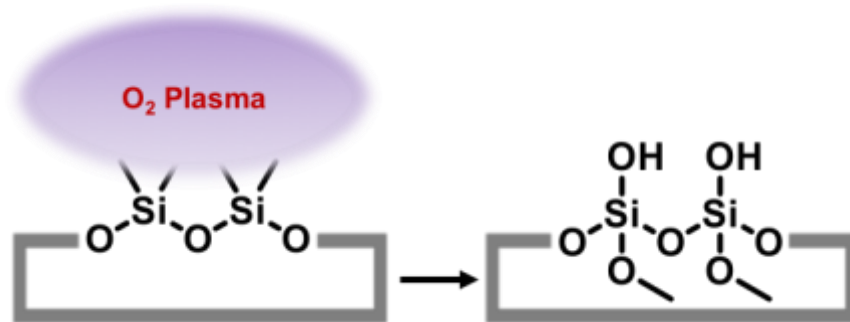


Figure 1.1 Oxygen plasma treatment for PDMS surface.

large amount of hydrophilic hydroxyl groups without cracking PDMS surface [18, 30]. Although UV/ozone treated PDMS also suffers from hydrophobic recovery like oxygen plasma-treated PDMS, Berdichevsky et al. [30] suggested that longer exposure time might reduce this effect.

Both oxygen plasma and UV/ozone treatments are simple and effective methods to improve the hydrophilicity of a PDMS surface, making them preferable choices for modifying short-term implants with microchannels [31]. While the hydrophilicity of the treated surface often suffers from the hydrophobic recover, even with additional treatment techniques, the energy treatments do not significantly improve other properties of the PDMS surface, such as friction coefficient or softness.

### **1.2.2 Teflon Coating**

Polytetrafluoroethylene (PTFE or Teflon) was first used as a urinary catheter coating in the 1960s and it has been used widely on latex catheters since then. The approach has the advantage of isolating less-biocompatible latex from surrounding tissues, generating less cytotoxicity than uncoated latex catheters. Nevertheless, the usage of Teflon coating on silicone catheters is uncommon since PDMS is much more biocompatible and less irritable than latex [32]. Even though the low frictional properties of the Teflon coating can minimize patient discomfort, its neutral charge and hydrophobicity may facilitate the adhesion of certain bacteria [19, 23]. In addition, SEM images reveal that Teflon-coated catheters are prone to cracking, which can occur during the coating process because of the high stiffness of the material [20]. Talja et al. [24] suggested that these deep cracks on the implant surface may induce toxicity.

### **1.2.3 Hydrogel Coatings**

#### **1.2.3.1 Radiation-induced Graft Method**

Radiation-induced graft hydrogels are widely used to modify biomedical implants. This approach uses UV radiation to generate free radicals on the PDMS surface, which act as graft sites for hydrogel monomers. Each hydrogel monomer must have one double carbon bond that can break and create two free electrons, one of which couples with a free radical to form a single carbon bond [8]. Hu et al. [33] demonstrated a one-step UV-induced graft polymerization to covalently bond hydrogels (e.g., PVA and PEG) to the PDMS surface, and successfully reduced the water contact angle to 45° on the grafted PDMS. Test results from Graiver et al. [20] also revealed a reduced friction on PVA hydrogel grafted catheters. The ultra-low surface friction is desirable as it can significantly improve patient comfort and eliminates the need for lubrication.

#### **1.2.3.2 Chemical Tailoring Method**

This emerging approach uses reagents (e.g., TMSPMA and APTES) as glues to link hydrogel chains to PDMS backbones. The reagents are covalently linked to the oxidized PDMS and subsequently linked to hydrogel chains via either carbon bonds or carbodiimide-mediated amide coupling [25, 26]. Zhang et al. [26] presented a PEG hydrogel coating on PDMS substrates by TMSPMA modification of the substrates. TMSPMA has double carbon bonds that would link with other monomers with the same bonds (e.g., crosslinker and PEG hydrogel) by forming new single carbon bonds. Despite the fact that PEG hydrogel has a higher Young's modulus than PDMS, the coated gel did not detach from the PDMS substrate after the substrate was bent by 90°. On the contrary, the PEG gel coating exfoliated easily without TMSPMA modification. The PEG-coated

PDMS also exhibits enhanced protein resistance and superior wettability, in comparison to native PDMS. Cha et al. [25] were the first to covalently bond alginate hydrogel to PDMS via carbodiimide-mediated amide coupling between the carboxyl groups on the alginate chains and the amino groups on APTES-PDMS. The resulting alginate-PDMS was more hydrophilic than native PDMS or OH-PDMS produced via oxygen plasma treatment.

### 1.3 Types of Hydrogels

Several notable hydrogels are introduced in the following sections and summarized in Table 1.2.

Types of Hydrogels	Applications and Properties
PVA	Popular in biomedical applications; coating for catheters [20, 34-36] Non-toxic and highly hydrophilic [34] May induce undesired cell adhesion; swelling affects durability [36, 37]
PEG	Biocompatible, hydrophilic, adjustable mechanical properties, low protein absorption [38-41] Anti-fouling coating for PDMS substrates [26]
PHEMA	Idea for bio-implants; common coating material for Foley catheters [19, 42, 43] Fair anti-fouling performance [43] Prone to cracking due to its stiffness [19]
Alginate	Great potential in biomedical applications due to its biocompatibility, low cost and ease of fabrication, but mechanically weak [44] Can be ionically and covalently crosslinked, but only the latter can be grafted on PDMS via chemical tailoring method [25, 45, 46] Ionically crosslinked alginate could achieve high strength at the cost of elasticity [47]
DN Hydrogels	Improve mechanical strength without sacrificing elasticity [48] Unlike co-polymers, two networks do not inter-crosslink [49]

**Table 1.2 A list of hydrogels for biomedical applications**

### **1.3.1 PVA Hydrogel**

Poly(Vinyl Alcohol) (PVA) is a promising biomaterial for contact lens, heart implants, tissue engineering and drug delivery applications, and it has been used as a coating material for urinary catheters to reduce the surface friction [20, 34-36]. PVA hydrogel has the advantages of being non-toxic and highly hydrophilic, and its uncomplicated chemical structure is simple for modifications. Although the bio-adhesive characteristic of PVA hydrogel is appreciated in tissue engineering applications, it could cause undesired cell adhesion onto the implants [36]. PVA hydrogel exhibits a high degree of swelling in biological fluid, which could ultimately result in delamination of the coating, raising concerns regarding implant durability [37].

### **1.3.2 PEG Hydrogel**

Poly(ethylene glycol) (PEG) has a simple structure and exhibits numerous desirable qualities, such as biocompatibility, hydrophilicity and highly adjustable mechanical properties through manipulation of its chemical content [38, 39]. Unlike PVA hydrogel, PEG hydrogel shows good resistance to protein absorption and does not support cell adhesion due to its low polymer-water interfacial energy, hydration layer, and steric repulsion [40, 41]. In the work of Zhang et al. [26], a thin layer of PEG hydrogel was grafted onto a PDMS surface by chemical modification. The fluorescent images and quantitative analysis showed significantly less protein adhering to the coated PDMS, when compared to a native PDMS surface.

### **1.3.3 PHEMA Hydrogel**

Poly(2-hydroxyethyl methacrylate) (pHEMA) is another common coating material for Foley catheters [19]. Like PVA and PEG hydrogels, pHEMA hydrogel is biocompatible and hydrated,

which also makes it an ideal candidate for contact lenses and artificial skins [42, 43]. Research conducted by Castillo et al. [43] also revealed that pHEMA has fair antifouling properties. Nevertheless, pHEMA coating is prone to cracking on softer substrates, to generate debris and attract bacteria [19]. Because each HEMA monomer has one double carbon bond, it can be grafted onto PDMS by either radiation-induced graft polymerization or chemical modification. Khorasani et al. [50] demonstrated an alternative method by using CO<sub>2</sub>-pulsed laser to introduce hydroperoxide groups as bonding sites. The coated surface showed increased resistance against platelet adhesion.

#### **1.3.4 Alginate Hydrogel**

Alginate, which is a natural polymer extracted from seaweed, has gained increasing attentions in biomedical applications such as tissue engineering, drug release, and artificial tissues, due to its inherent biocompatibility, low cost, and ease of fabrication [44]. Alginate monomers can be crosslinked by either covalent bonding in the presence of crosslinkers or by divalent ions like Ca<sup>2+</sup> [45, 46]. Generally, alginate has weak mechanical strength that does not allow load bearing [44]. Kuo and Ma [47] claimed that the mechanical strength of ionically crosslinked alginate gel could be improved with slower gelation rates and increased alginate concentrations; however, the increased compressive modulus that would result from the higher monomer content would be undesirable for coating applications.

#### **1.3.5 DN Hydrogels**

The double network structure was first proposed by Gong et al. [48] in a search for super tough and highly hydrated polymers for biomedical applications. They managed to improve poly(AMPS-

co-TFEA) hydrogel's fracture stress by more than 300-times without sacrificing the hydration content and the fracture strain, by incorporating PAAm as a second network. Differing from copolymer hydrogels, DN hydrogels are synthesized via a two-step cast process, and the two networks do not inter-crosslink. Gong et al. [48] compared the two networks to bone and flesh, respectively, and postulated that the first network should be rigid and brittle, while the second network would be soft and ductile, so that the soft network would evenly distribute the load onto the first network [49]. This idea was challenged by Sun et al. [37] who proposed a super stretchable DN hydrogel using soft alginate as the first network and polyacrylamide as the second network. The alginate network was ionically crosslinked and the second network was covalently crosslinked with MBAA. Interestingly, both networks were further joined together by covalent crosslinks between amino groups. The resulting DN was 20-times more stretchable and had a fractural energy that was comparable to natural rubber. Unfortunately, this formulation could not be used as a coating for PDMS-based implants because the ionically crosslinked alginate cannot be grafted onto a PDMS surface.

#### 1.4 DN Alginate-pHEMA Hydrogel Coating

In this project, a novel hydrogel coating for PDMS implants was developed based on a double-network structure (Figure 1.2). This is the first time that natural alginate and synthetic pHEMA are used to construct a double-network hydrogel as coating material for PDMS-based implants. Both hydrogels are synthesized via covalent crosslinking, but the two networks are not inter-crosslinked. The alginate hydrogel is used to fabricate the first network as a scaffold, and the pHEMA forms a denser network within the pores of the alginate; both networks are highly biocompatible [44, 51]. A cytotoxicity experiment was conducted to confirm this claim. Although the coating is designed primarily for urinary catheters in urethral or suprapubic applications, it can also be applied onto other biomedical implants, such as cardiac catheters and implantable drug delivery devices.

The coating has a thickness of 0.25-0.35 mm when cast and can be cast onto PDMS surfaces of any shape. It is thicker than most previously proposed hydrogel coatings, creating a soft “cushion” between the coated PDMS implant body and delicate tissues [26, 52]. Unlike previously proposed hydrogel coatings for PDMS implants, our design incorporates a distinct second-network of

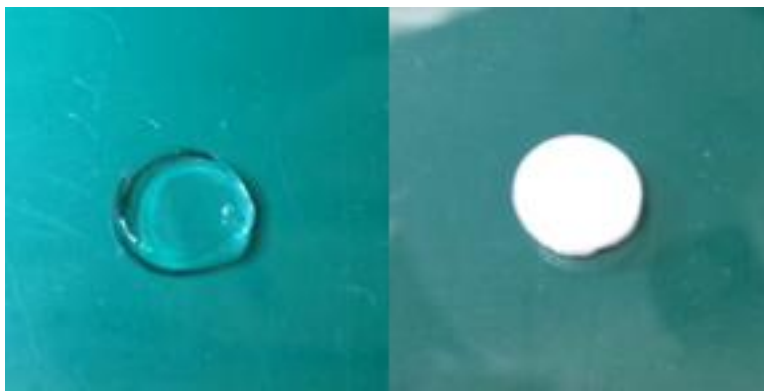


Figure 1.2 SN alginate gel (left) and DN alginate-pHEMA gel (right).

pHEMA to improve alginate gel's mechanical strength without sacrificing its elasticity. The adhesion strength of the coating on a PDMS substrate is enhanced by chemical modification and micropillar anchors to ensure the coating stability during insertion and removal of an implant. For demonstration and ease of fabrication purposes, all the micropillar PDMS substrates and bare PDMS substrates used in this project were flat. The DN gel coating is designed to possess ultra-low friction and softness comparable to urethral tissues, to improve the patient's comfort and minimize the chance of mucous membrane injury.

## **1.5 Thesis Overview**

This thesis is presented with an introductory chapter, two chapters of experimental methods and discussions, and a conclusion that summarizes the current work and suggests potential future directions.

Chapter 1 briefly reviews the background of PDMS in biomedical applications, including its advantages and drawbacks when used as an implant material. Different surface modification techniques are described, including energy treatments and polymer coatings for PDMS-based devices and implants. The deficiencies and challenges of existing methods are explained, and a double-network (DN) alginate-pHEMA hydrogel coating is proposed to resolve these problems.

Chapter 2 provides an overview of the design, synthesis, and characterization of the proposed DN hydrogel, with a discussion of the experimental results. First, the polymerization mechanisms of the first network alginate hydrogel and the second network pHEMA hydrogel are discussed with regards to the double network structure. Then, the step-by-step fabrication process is demonstrated, and the DN gel's mechanical properties are investigated by adjusting the key ingredients, such as

crosslinker and monomer concentrations. After optimizing the formulation, the surface morphology and internal microstructure of a single network (SN) alginate hydrogel was reviewed by SEM and compared to the finalized DN gel. This is followed by the evaluation of the swelling coefficient and cytotoxicity of the SN and the finalized DN hydrogel.

Chapter 3 focuses on the formation of DN gel coatings on PDMS substrates and the characterization of both hydrogel-coated and bare surfaces. This chapter begins with the design and fabrication of micropillar PDMS substrates, followed by the chemical modification process for the substrates, and ultimately, the hydrogel coating fabrication. Coating adhesive strength is investigated by a shear test, and the data for micropillar and bare substrates is compared to evaluate the effectiveness of micropillar anchors. Finally, the friction coefficient and water contact angle of DN gels, lubricated PDMS, and bare PDMS are measured, and the results are discussed.

Chapter 4 summarizes this thesis and suggests possible directions for future development of the proposed coating.

## Chapter 2: Double-Network (DN) Alginate-pHEMA Hydrogel

### 2.1 Polymerization Mechanism

Alginate-pHEMA gel is prepared via a two-step network formation method. Alginate hydrogel is synthesized to form the first network that defines the geometry of the DN alginate-pHEMA gel (Figure 2.1a). Subsequently, the cured alginate gel is incubated in the solution containing HEMA monomers, crosslinker, and photoinitiators to allow diffusion of the solutes into the alginate network (Figure 2.1b). HEMA monomers are polymerized with the crosslinker MBAA to form the pHEMA network and occupy the interstitial space within the alginate network (Figure 2.1c).

#### 2.1.1 Alginate Network

Ionic crosslinking and covalent crosslinking are two of the most commonly used polymerization methods for alginate gels [44]. The former method uses divalent cations (i.e.,  $\text{Ca}^{2+}$ ) to create junctions between  $\alpha$ -L-guluronate blocks of alginate chains, resulting with the gel structure [45]. Calcium chloride ( $\text{CaCl}_2$ ) is one of the most commonly used ionic crosslinkers for alginate, and polymerization is initiated by adding alginate pre-gel solution into a  $\text{CaCl}_2$  aqueous solution; however, the high solubility of such agents results in rapid gelation and an inhomogeneous network [53]. The gelation rate is thus crucial for the structural uniformity, which ultimately affects the mechanical strength of the resulting gel. Researchers [47, 54] demonstrated that crosslinking agents with very low solubility in pH-neutral water, such as  $\text{CaCO}_3$  and  $\text{CaSO}_4$ , can initiate a more gradual gelation in the presence of Glucono- $\delta$ -lactone (GDL) that helps form a uniform gel structure with more consistent mechanical properties.

As shown in Figure 2.1d, the covalent crosslinking technique uses a crosslinker molecule, such as AAD instead of divalent cations, to create carbodiimide-mediated amide coupling between

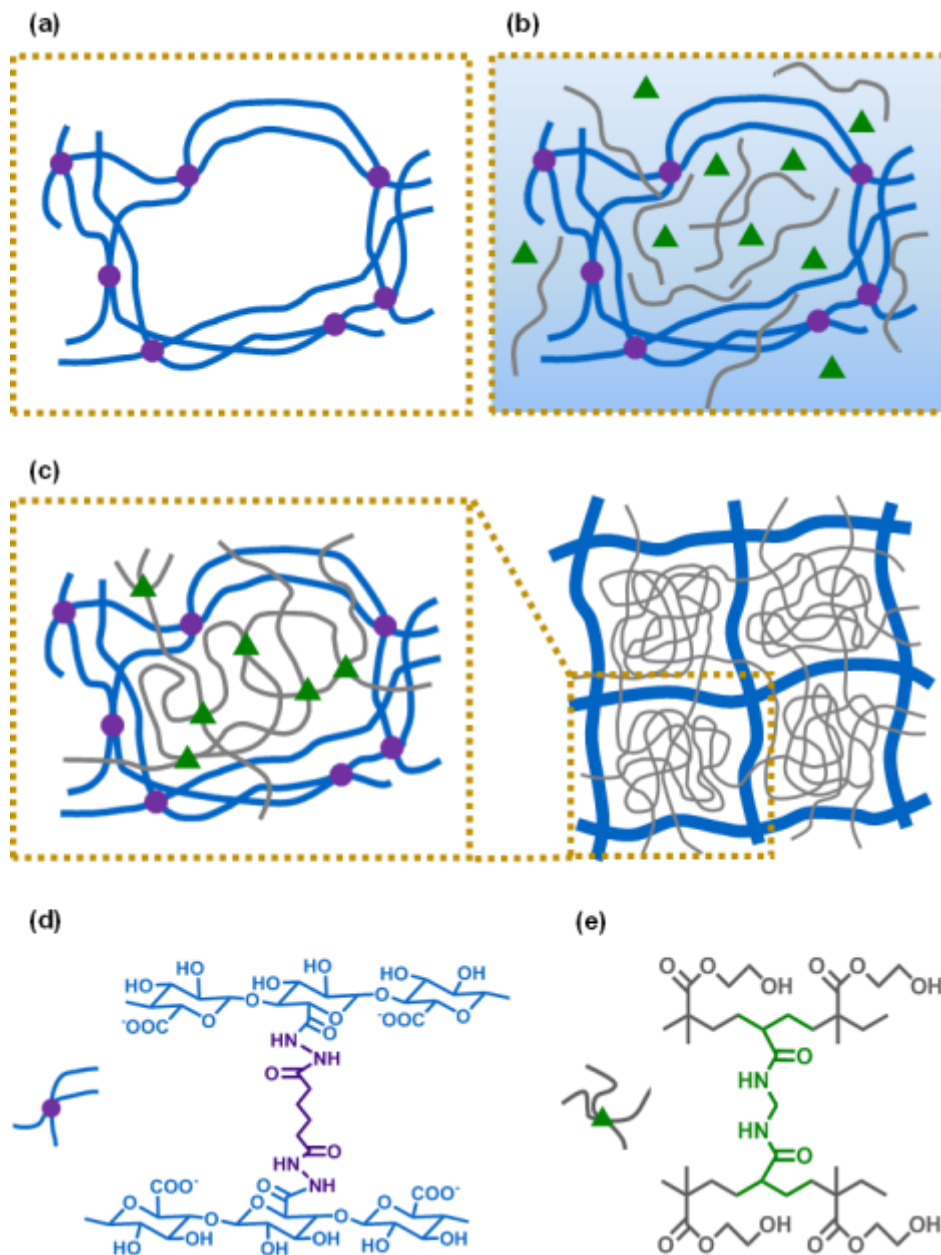


**Figure 2.1** Schematics of the two networks of alginate-polyHEMA hydrogel; (a) alginate network, (b) diffusion of HEMA monomers, (c) resulting DN structure, (d) alginate chains covalently crosslinked by AAD (purple circles), (e) HEMA monomers covalently crosslinked by MBAA (green triangles).

alginate chains that leads to the gel structure. The coupling is established via a three-step sequential chemical reaction: 1) water-soluble carbodiimide EDC reacts with a carboxylic acid group on the alginate chains to form an active intermediate; 2) NHS is introduced to improve the creation efficiency and form NHS esters; and 3) this more stable intermediate allows for the efficient conjugation to AAD [46, 55].

The covalently crosslinked alginate hydrogel has three significant advantages over the ionically crosslinked gel when being used as a coating material for PDMS devices. First, the ionically crosslinked gel is less stable in physiological conditions due to the dissolution of the alginate network caused by the escape of  $\text{Ca}^{2+}$  in the presence of phosphate, citrate, lactate,  $\text{Na}^+$ , and  $\text{Mg}^{2+}$  [55, 56]. Secondly, the stress of the ionically crosslinked alginate gel relaxes through dissociation and reforming of crosslinks, causing irreversible plastic deformation. Covalently crosslinked alginate gel, in contrast, relaxes the stress through migration of water within the network, leading to elastic deformation [57]. Finally, unlike covalently crosslinked gel, the ionically crosslinked gel cannot form either ionic or chemical bonds with PDMS substrates during gelation, thus leading to a more secure bonding between the two materials [25].

### **2.1.2 PHEMA Network**

We chose MBAA as the covalent crosslinker for the pHEMA network because of its acceptable hydrophilic property and commercial availability, though the CBMA-based dimethacrylate crosslinker, CBMAX, has been reported to have superior solubility and non-fouling properties compared to MBAA. The CBMAX crosslinker must also be custom-synthesized via a series of complex chemical reactions [58, 59]. HEMA and MBAA monomer units are attached via addition polymerization, where an active initiator attaches to one of the electrons in the double carbon bond,

and the other electron forms a new single carbon bond with another electron from the double carbon bond in the neighboring monomer unit [60]. Because each MBAA unit possesses two double carbon bonds, it forms a junction with four HEMA units; thus, causing the polymer to exhibit the network structures.

## 2.2 Hydrogel Preparation

### 2.2.1 Single-Network (SN) Alginate Hydrogel

Medium viscosity sodium alginate salt (Sigma-Aldrich, St. Louis, MO, USA) was dissolved in the 100 mM MES buffer at 1.5 wt-%. The alginate solution was agitated thoroughly by a magnetic stirrer at 700 RPM for 24 h, and its pH was adjusted to 5.0 by HCl or NaOH if necessary. The pre-gel solution was mixed with EDC and NHS and covalently cross-linked with AAD (molar ratio of alginate monomer:EDC:NHS:AAD = 4:6:3:1) [55]. EDC was added first, and NHS was added 8 min later. AAD was added 6 min after NHS. The mixture was agitated for 30 s on a water mixer after each ingredient was added. Before the pre-gel mixture was transferred to the PDMS substrate,

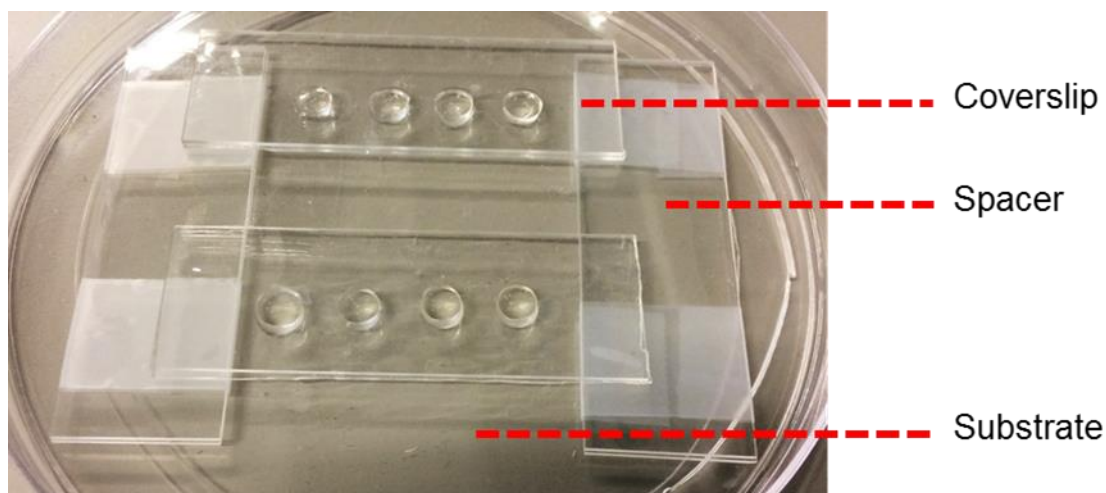


Figure 2.2 Fabrication setup for SN alginate hydrogel dishes.

it was further agitated in a sonicated bath for 30 s. The single-network gel dishes, each made from approximately 100  $\mu$ l of the previously described alginate pre-gel solution, were assembled between the PDMS substrate and the PDMS-coated glass coverslips (Appendix A), and the substrate and the coverslips were separated by 2-mm spacers (Figure 2.2). After curing at room temperature for 4 h, the entire setup was immersed in distilled water for 30 s, and then the gel dishes were carefully removed from the substrate with a razor blade. The gels were incubated in PBS solution to reach the swelling equilibrium before being subjected to any test; incubation was not required if they were used to prepare DN gels.

### **2.2.2 Double-Network (DN) Alginate-pHEMA Hydrogel**

Double-network alginate-pHEMA hydrogels with various concentrations of second network monomer (HEMA) and crosslinker N,N'-methylene bisacrylamide (MBAA) were prepared to study the correlation between the mechanical properties of the hydrogel and its second network and crosslinker concentrations. Initially, the concentration of HEMA monomer was fixed at 2M, and the crosslinker concentration was increased from 0 to 0.5, 1, 2.5, and then to 4 mol-%. Then, the crosslinker concentration was fixed at 2.5 mol-%, then the amount of HEMA monomer was changed from 1 to 2 and then to 3 M. SN hydrogel samples were incubated in the HEMA monomer solutions for 24 h and exposed to 365 nm UV light for 20 min on each side. The resulting DN hydrogel dishes were rinsed with 70% ethyl alcohol and DI water, and then immersed in PBS solution for 36 h prior to the compression test. Details are shown in Appendix B.

## **2.3 Characterizations**

### **2.3.1 Analysis of Mechanical Properties**

The ultimate compressive stress and strain of SN alginate hydrogel and alginate-pHEMA DN hydrogel were measured by a Mach-1 mechanical testing system (Biomomentum, Laval, QC, Canada). The dimensions of each gel dish were measured by a caliper prior to the test. The upper compression plate of the machine was manually lowered until it was approximately 3 mm away from the sample. The machine was then set to ‘find contact,’ which allowed the compression plate to be lowered at a rate of 0.1 mm/s until a resistance of 0.075 N was sensed. During the compression, the samples were compressed at a rate of 0.01 mm/s, and the travel distance of the compression plate was set to be 80% of each sample’s thickness to avoid machine damage. Three repeats were conducted for each formulation.

Separately, 3 mm-thick SN and DN (2M HEMA and 2.5mol% MBAA) hydrogel cylinders were fabricated using the aforementioned techniques and immersed in PBS solution to reach swelling equilibrium prior to the test. As shown in Figure 2.3, hydrogel samples were placed on a height-adjustable platform, directly underneath a cutter with rounded edge. The platform was gradually raised until the cutter sliced through the samples to qualitatively investigate how well the hydrogels resisted uneven compression.

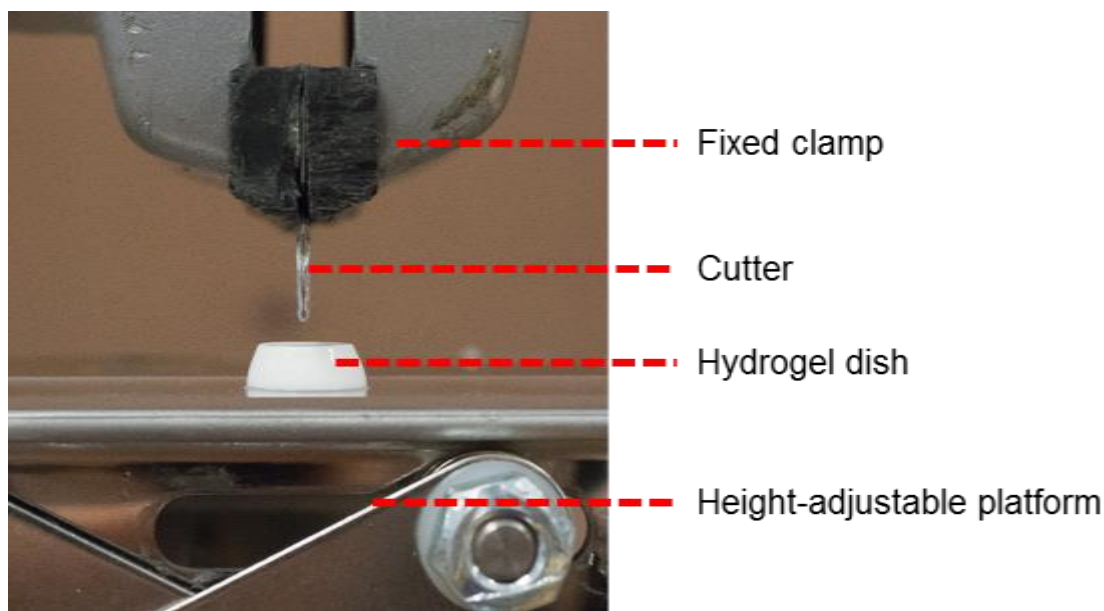


**Figure 2.3 Setup for hydrogel slicing experiment.**

### **2.3.2 Swelling Coefficient and Water Content Comparison**

Single-network hydrogel droplets, each made from approximately 100  $\mu\text{l}$  1.5 wt-% alginate pre-gel solution (molar ratio of alginate monomer:EDC:NHS:AAD = 4:6:3:1), were cured at room temperature for 4 h on a PDMS plate. Three samples were then removed from the substrate and immersed in PBS solution until they reached equilibrium swelling state. Meanwhile, the remaining samples were soaked in 10vol% ethyl alcohol solution of various amount of HEMA monomers (1 M, 2 M, or 3 M) containing 0.5 wt-% Irgacure 651, 1 wt-% Irgacure 2959 and 2.5 mol-% MBAA for 24 h. Subsequently, samples were exposed to 365 nm UV light for 40 min, and then immersed in PBS solution until their swelling reached equilibrium. The weight of each SN and DN sample was measured every 6 or 12 h.

The swelling coefficient of hydrogel was determined as:

$$\text{S. C.} = 100\% \times \frac{m_t}{m_0} \quad (1)$$

where  $m_0$  and  $m_t$  are the initial mass of the hydrogel and the mass of the swollen hydrogel at t-th hour, respectively. Subsequently, both SN and DN hydrogel samples were dried on a 50°C heater for 24 h. The dehydrated hydrogel samples were weighed, and the water content value was determined as:

$$W.C. = 100\% \times \frac{m_f - m_d}{m_f} \quad (2)$$

where  $m_f$  and  $m_d$  are the final mass of the wet hydrogel and the mass of the dehydrated hydrogel, respectively.

### 2.3.3 Cytotoxicity Study

This experiment was conducted in collaboration with Axel Chu. We incubated HEK cells in the culture media with SN hydrogel, DN hydrogel, or the control, and then evaluated the biocompatibility of these gels by analyzing the HEK cells' growth rates, as determined by the percentage area of confluence.

SN and DN (2 M HEMA, 2.5mol% MBAA, 0.5 wt-% Irgacure 651 and 1 wt-% Irgacure 2959) gel dishes, each made from 200  $\mu$ l 1.5 wt-% alginate pre-gel solution (molar ratio of alginate:EDC:NHS:AAD = 4:6:3:1), were cast using the spacer method from Section 2.2 (spacer thickness = 1 mm). After polymerization of the second network of the DN gel, the DN gel dish was washed thoroughly with 70% ethyl alcohol and DI water. They were then immersed in PBS solution to reach swelling equilibrium, and the solution was changed every 4 h during the first 24 h. Subsequently, the samples were transferred to a laminar flow clean bench and sterilized with 70% ethyl alcohol. To remove any residual ethyl alcohol, each sample was washed in 100 ml of sterile PBS solution for 20 min three times.

Separately, wells of a standard six-well cell culture plate were seeded with HEK cells ( $4.5 \times 10^5$  cells per well), and each well was filled with 9 ml cell culture medium (DMEM/F-12 medium supplemented with 10% fetal bovine serum and penicillin/streptomycin). 40  $\mu\text{m}$  sterile cell strainers (Fisher Scientific, New Hampshire, USA) were used to prevent the gel samples from contacting the bottom of the wells where the cells were proliferating. The sterilized gel samples were individually suspended in the cell culture medium by strainers in the wells. Meanwhile, an empty strainer was placed in another cell-seeded well as the control. The cells and gel samples were incubated in the described medium at  $37^\circ\text{C}$  with 5%  $\text{CO}_2$  for six days without change in medium, and photos of the cells were taken at six locations in each of the wells every 24 h by an Olympus IX81 Cel-TIRF microscope at  $20\times$  magnification. The coordinates for each location were saved in the microscope, allowing photos to be taken at the same location on the following days. Using ImageJ software, we analyzed the percentage area confluence based on the microscope images. Step-by-step instructions for operating the software are shown in Appendix C.

## **2.4 Results and Discussion**

### **2.4.1 Mechanical Properties**

The mechanical properties of DN hydrogel depend highly on the concentration of HEMA monomer and crosslinker MBAA. When the HEMA monomer concentration is fixed at 2 M, the crosslinker MBAA composition was increased from 0 to 0.5, 1, 2.5, and 4 mol-%. The Young's modulus is based on the average slope of the lower portion of the stress-strain curve ( $<30\%$ ) (Figure 2.4a). As shown in Figure 2.4b, the presence of the pHEMA network and the increasing crosslinker concentration results in a decrease in hydrogel elasticity. The DN gel's fracture stress improves with crosslinker concentration before 2.5 mol-%, and it decreases afterward (Figure

2.5a), a trend that does not conform to the model presented by Gong et al. [48] due to different crosslinking mechanisms for the two networks. Some samples fractured under significantly lower loads, compared to others, showing uneven fracture patterns, and more of these premature fractures were observed among samples containing 4 mol-% crosslinker. The higher crosslinker content may result in more rapid gelation that disrupts the formation of the homogenous second network, so that the samples containing 4 mol-% crosslinker had lower fracture stress than those containing 2.5 mol-% crosslinker [61]. We also noticed that the custom-made upper compression plate experienced some unavoidable slippage since the less-than-perfect fit of the upper compression plate led to a small degree of misalignment between the compression plates before the gels fractured. Unlike Young's modulus and fracture stress, the fracture strain for all formulations scatters in a range between 0.66 and 0.738 and does not show a direct correlation with crosslinker content (Figure 2.5b). Although softness and elasticity is favorable, mechanical strength is required for handling; hence, we chose 2.5 mol-% as the final crosslinker concentration since it offered the highest fracture stress at  $502.04 \pm 14.41$  kPa without a drastic loss in elasticity.

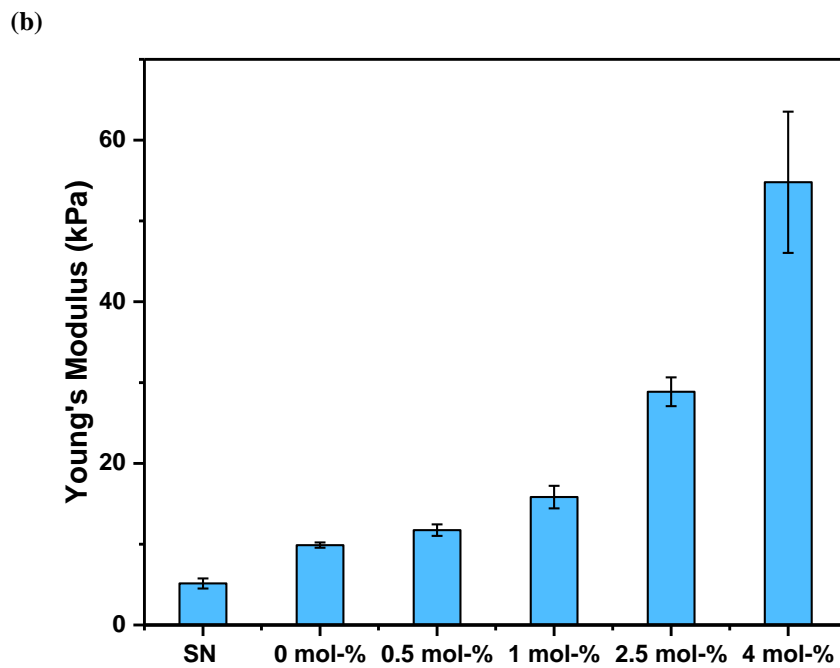
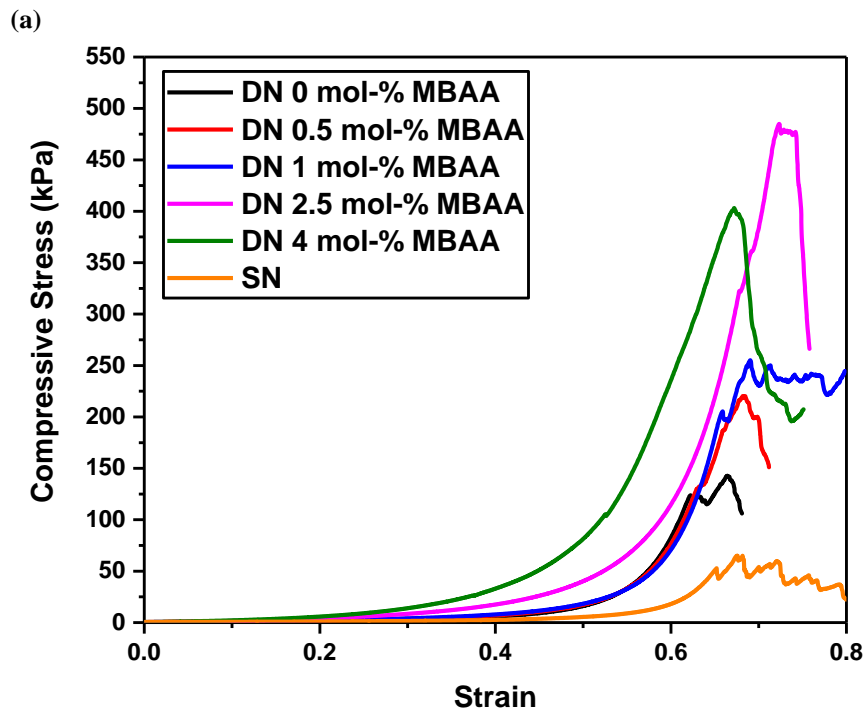


Figure 2.4 (a) Stress-strain curves and (b) Young's modulus.

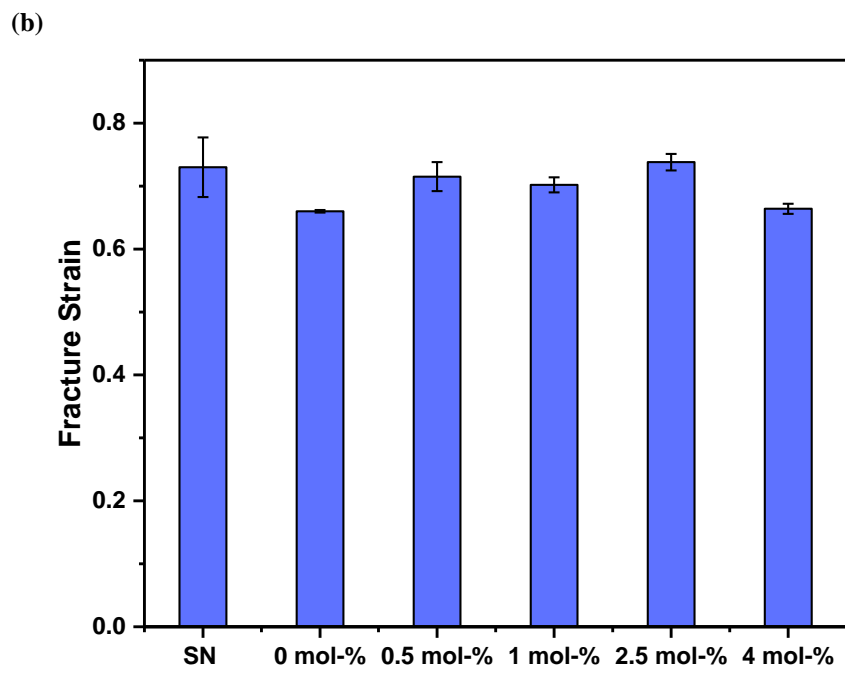
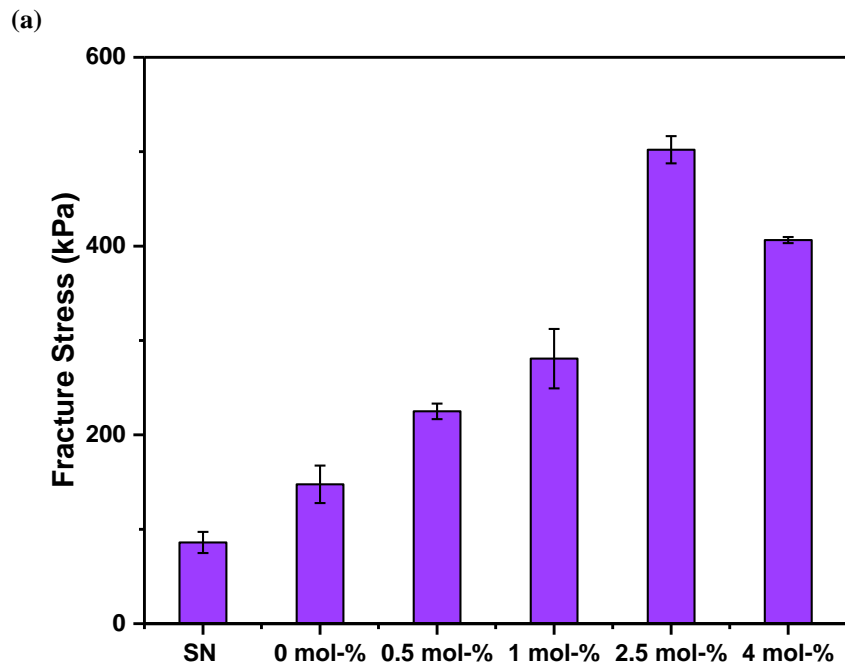


Figure 2.5 (a) Fracture stress and (b) fracture strain.

Subsequently, we fixed the crosslinker MBAA content at 2.5 mol-% and adjusted the HEMA monomer concentration from 1 to 2 and then to 3 M. Figure 2.6a shows the stress-strain curves with varied monomer concentrations, and Figures 2.6b and 2.7a summarize the Young's modulus and fracture stress for all formulations, respectively. Both fracture stress and Young's modulus show improvements with increased HEMA monomer concentrations, which is attributed to the increased network density and entanglement, though neither the correlation is linear. The DN gel containing 1 M HEMA only demonstrates a slight improvement over the alginate gel in fracture stress and Young's modulus, while the 2 M HEMA formulation had 302.08% and 310.53% increases in these two properties over the 1 M HEMA formulation, respectively. With a Young's modulus of  $28.86 \pm 1.78$  kPa, the DN gel that contained 2 M HEMA was exceptionally close to resembling the elasticity of urethral tissue (10-20 kPa), which would be a desired quality for bioengineering applications [62, 63]. Although the gel containing 3 M HEMA was the strongest among all formulations, the improvement over the 2 M HEMA formulation was marginal, and it had a drastically higher Young's modulus of  $87.53 \pm 16.10$  kPa, which is three times higher than that of urethral tissue. A compromise between mechanical strength and elasticity is necessary in determining the final formulation, and the 2 M HEMA formulation (2.5 mol-% crosslinker) is considered the preferable choice for use as a coating material for urinary catheters. As seen in Figure 2.7b, the HEMA monomer content does not significantly affect the fracture strain of DN gels. Initially, the weak presence of the pHEMA network (1 M HEMA formulation) results in a lower fracture strain than the alginate gel; however, a marginally improvement is seen with the increasing polyHEMA network density. The DN gels, with 2 M and 3 M HEMA content, have similar fracture strains ( $0.74 \pm 0.01$  and  $0.78 \pm 0.08$ , respectively) to that of the SN gel ( $0.73 \pm 0.05$ ).

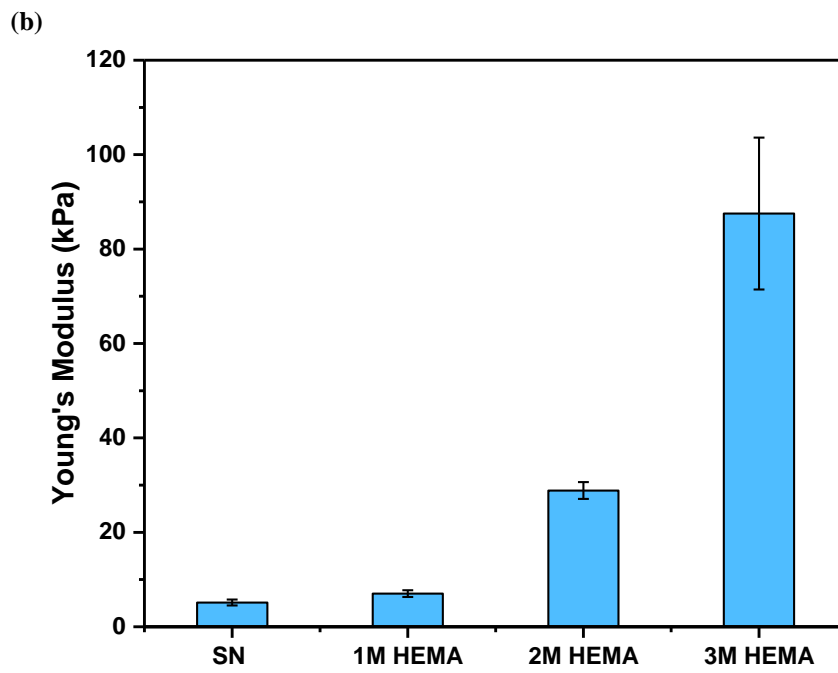
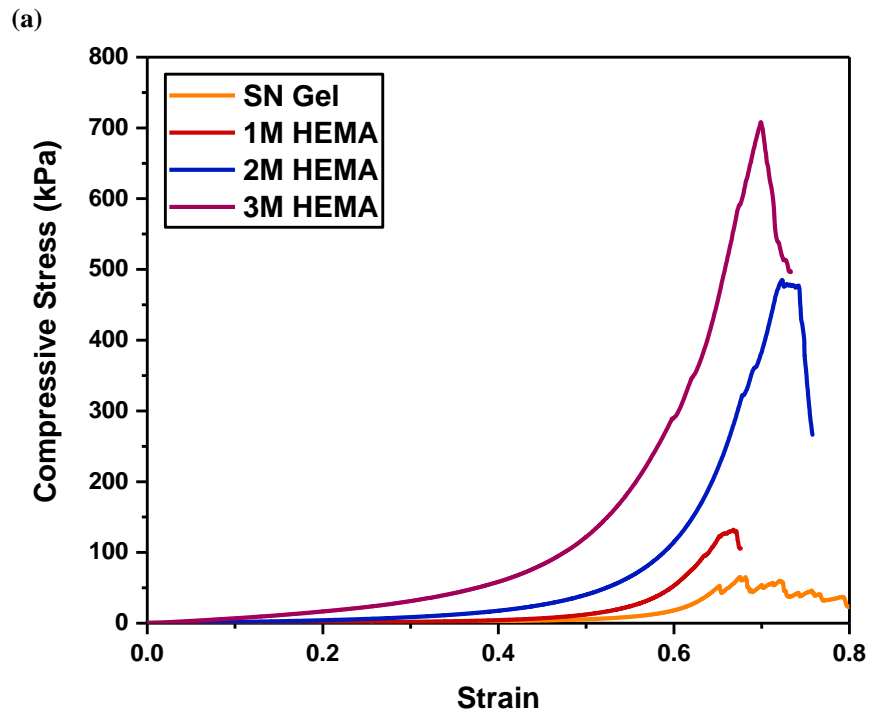
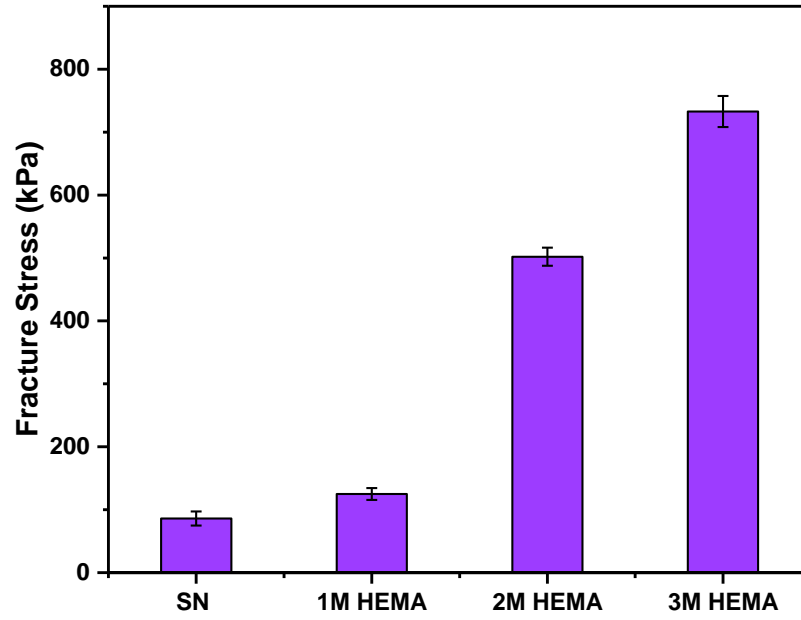


Figure 2.6 (a) Stress-strain curves and (b) Young's modulus.

(a)



(b)

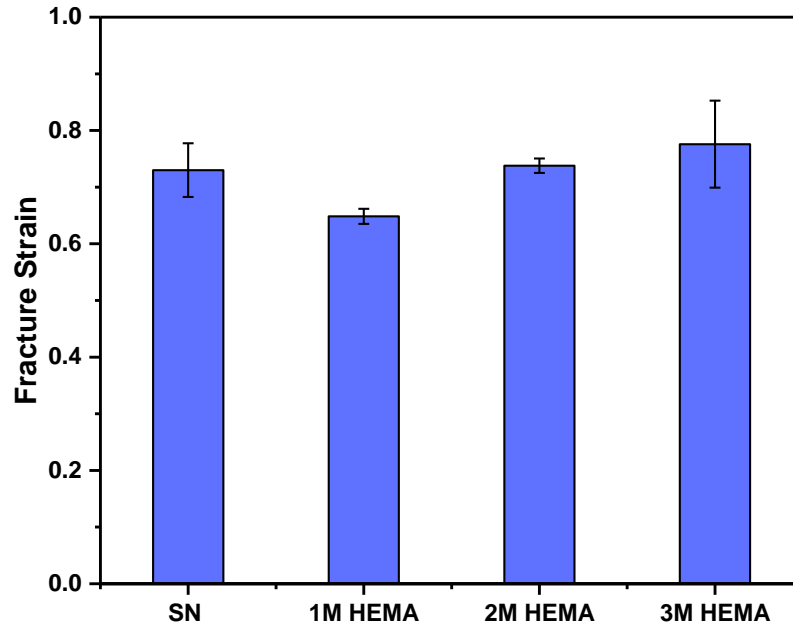


Figure 2.7 (a) Fracture stress and (b) fracture strain.

Only three monomer concentrations were explored since material optimization was not the ultimate objective of this project. Furthermore, the gel dishes had already experienced a certain degree of dehydration after incubation in the 3 M HEMA monomer solution; a higher monomer

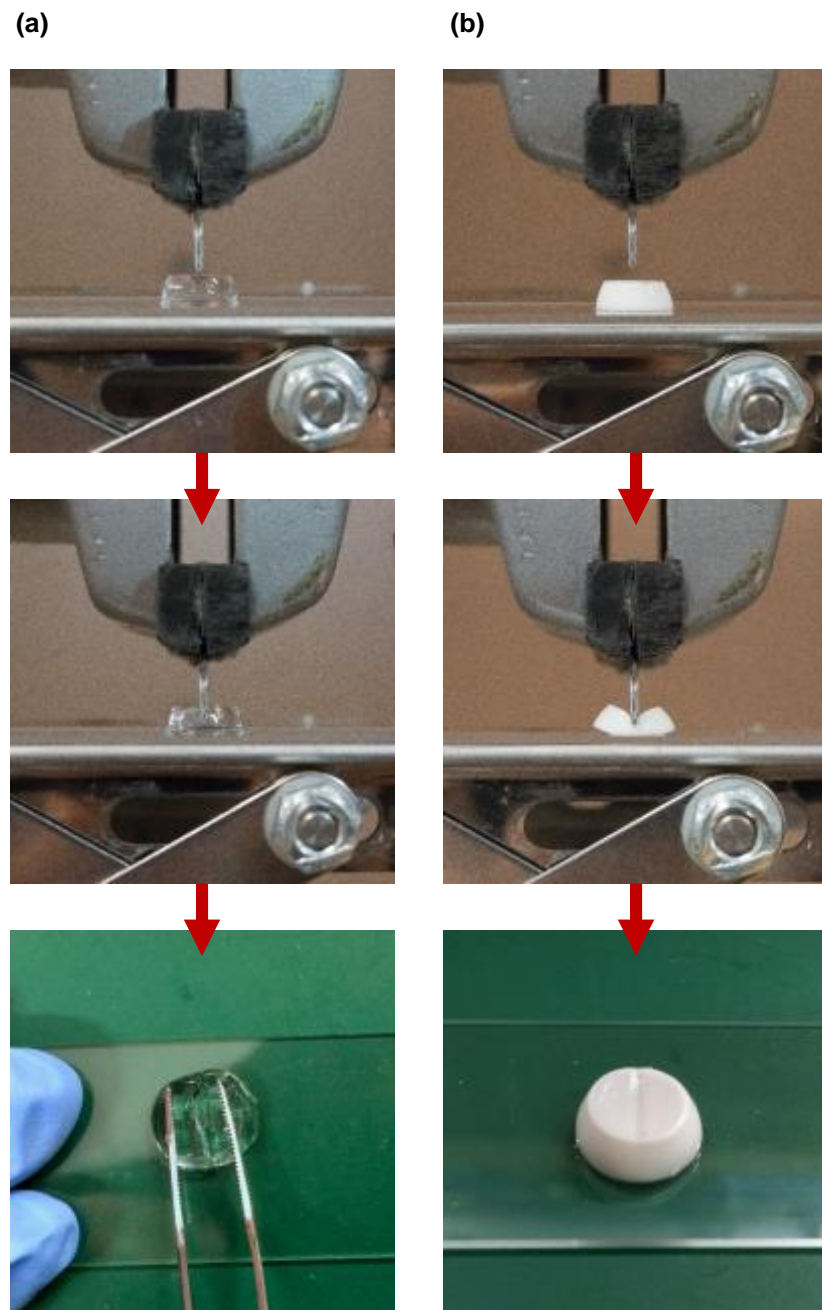


Figure 2.8 Slicing resistance of (a) SN alginate gel and (b) DN alginate-pHEMA gel.

content would severely deform the hydrogel structures. Finally, during the preparation process for the HEMA monomer solution, the solution containing 1 M HEMA turned cloudy after distilled water was added; presumably because of Irgacure 651 precipitation. Such phenomena were not observed in the 2 M and 3 M formulation solutions; hence, we conclude that the HEMA monomer improves the solubility of Irgacure 651 in aqueous solution and we would not advise a further decrease in the HEMA content below 1 M.

Slicing resistance of both the SN alginate gel and the DN gel was evaluated by comparing their local fracture strains that resulted from a cutter. Figure 2.8 shows that the SN alginate gel cylinder fractures at a strain of approximately 50 %. On the other hand, the DN gel (2 M HEMA and 2.5 mol-% MBAA) can still retain its structural integrity under 65% strain and can return to its original shape without noticeable plastic deformation. Even though the SN and DN gels have nearly identical fracture strains under even compressive loads (Figure 2.7b), the latter exhibits a roughly 30% higher fracture strain than the SN gel when compressed by the cutter; this quality of DN gel has made it preferable since even compression rarely exists in real-life situations.

#### **2.4.2 Microstructure**

SEM images of freeze-dried SN and DN (2 M HEMA and 2.5 mol-% crosslinker) hydrogels, taken at random locations across the surface and cross-sections of the gel dishes, are presented in Figure 2.9. No discernible porous network is perceived on the surface of SN or DN gel samples, as shown in Figure 2.9a-1 and 2.9b-1, respectively; whereas, they exhibit distinct textures, where the DN gel surface has unique wrinkle patterns, presumably resulting from the dehydration during the incubation process in HEMA monomer solution. Only the morphology of the surfaces molded by

PDMS coverslips were investigated in this thesis since DN hydrogel coating is cast underneath coverslips.

Figure 2.9a-2 shows a well-defined porous network on the cross-section of SN hydrogel under 50 $\times$  magnification. The SN gel forms a honeycomb structure with random orientations, as can be seen in the center and the upper right side of the image. Moreover, an obvious difference in pore size is observed in the same hydrogel sample, indicating the existence of an inhomogeneous network. On the other hand, the cross-section of DN is smooth and dense under the same magnification (Figure 2.9b-2). Although the DN gel is synthesized by polymerizing HEMA monomers within the SN gel, the pores of alginate network in the DN gel are significantly smaller than those in the SN gel (Figure 2.9a-3 and 2.9b-3). The difference between the alginate network pore sizes in SN and DN gels is primarily the result of the aforementioned dehydration during incubation and swelling of the SN gel in PBS solution (the swelling property will be discussed in Section 2.4.3). The locations of these images could also play a role, since we know from Figure 2.9a-2 that the size of the pores in the SN gel vary largely from 20  $\mu\text{m}$  to 200  $\mu\text{m}$ , and the size of the photographed alginate network pores in DN ( $\sim 30$   $\mu\text{m}$ , Figure 2.9b-4) fits well within this range.

The alginate network and the pHEMA network exhibit distinct morphologies within the DN hydrogel body, where long-chain sodium alginate salt monomers form honeycomb-like scaffolding that defines the geometry of DN gel, and short-chain HEMA monomers form a much finer network within the pores of alginate network, resulting in a nested structure (Figure 2.9b-4). The alginate gel is soft and weak, and the pHEMA alone is unable to crosslinker properly in the cast, resulting in phase separation, and gelation only occurs at the bottom of the cast. Nevertheless, within the micro pores of the alginate network, HEMA can polymerize properly and improve

mechanical properties of the resulting DN gel. According to Gong et al. [49], the improved toughness is attributed to stress release caused by the fracture of the more brittle network.

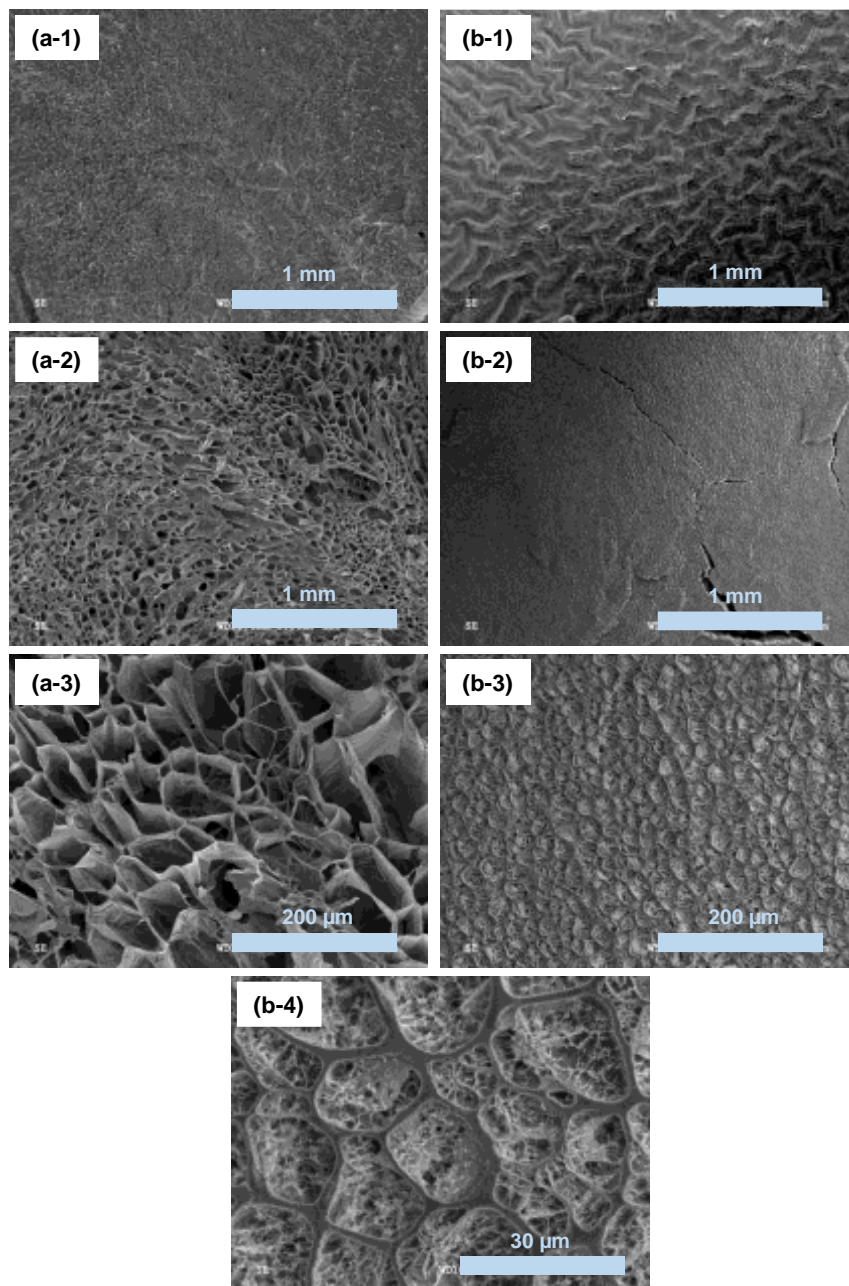


**Figure 2.9 (a) SN alginate hydrogel and (b) DN alginate-pHEMA hydrogel; (1) 50× magnification on the surface, (2) 50× magnification on the cross-section, (3) 250× magnification on the cross-section, and (4) 1500× magnification on the cross-section.**

### 2.4.3 Swelling Coefficient and Water Content

Figure 2.10a shows the equilibrium swelling coefficient of SN gel and DN gels with various pHEMA network densities, calculated from Equation (1). The incorporation of the pHEMA network drastically reduces the swelling of hydrogels in PBS solution. A decrease in overall mass is observed for all DN gels after the first 6 to 12 h, which could result from unreacted chemicals leaching out. Subsequently, both 1 M and 2 M HEMA formulations showed minor swelling, while the 3 M formulation did not swell at all. The equilibrium swelling coefficient decreases with an increase in the pHEMA content. Furthermore, DN gels of all formulations reached equilibrium swelling after 24 h of incubation, which was significantly faster than the SN gel (~ 84 h). As we expected, the presence of the pHEMA network largely restrains the swelling of the DN hydrogel, which believe to be a desired property for coating applications since a large degree of swelling can cause delamination of the gel coating and absorption of biomolecules (e.g., proteins) [43].

The high water content makes hydrogels attractive candidates for bioengineering applications, because it tends to mimic biological tissues and it can reduce the contact surface friction [51, 64, 65]. The equilibrium water content for SN gels and DN gels with various pHEMA network densities was calculated from Equation (2) and presented in Figure 2.10b. The SN gel has the highest water content thanks to its larger pore size; and the hydration level gradually decreases with increasing pHEMA network density as pHEMA polymerizes within the pores of the alginate network and disperses the water inside. At  $66.54 \pm 0.61\%$ , the 3 M pHEMA DN gel is the least hydrated formulation, though its water content is still considered ‘high’ for medical implants (e.g., contact lenses). Our finalized formulation (2 M pHEMA) has an exceptional water content of  $77.09 \pm 0.61\%$ , without suffering from the poor mechanical properties.

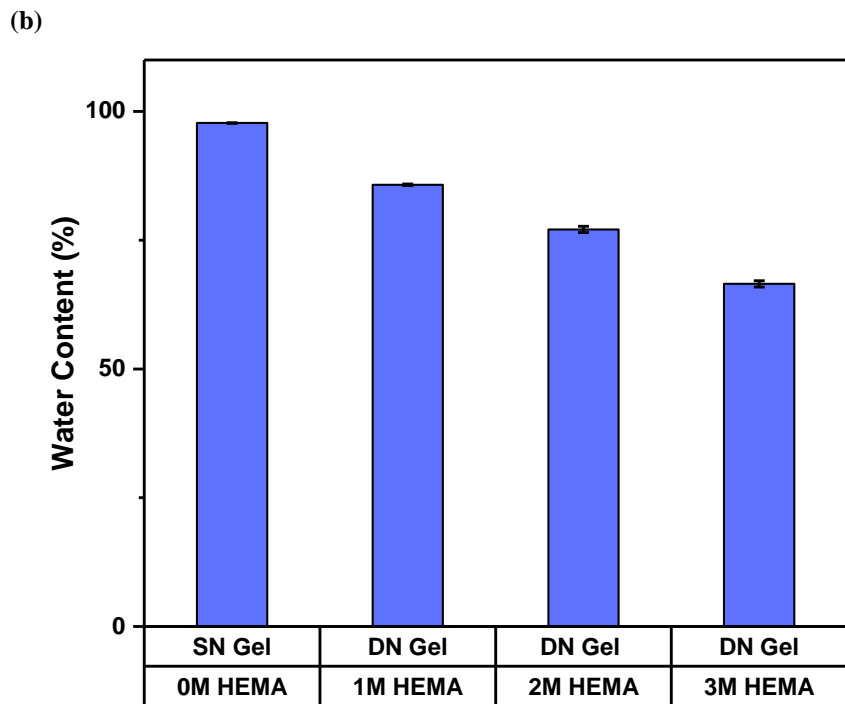
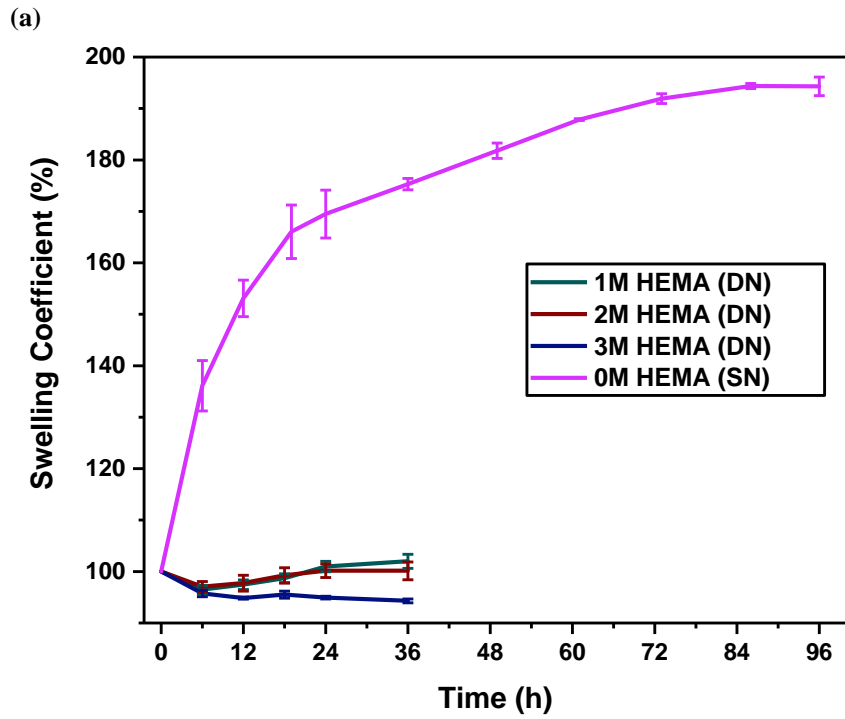


Figure 2.10 (a) Swelling coefficient and (b) equilibrium water content.

#### 2.4.4 Cytotoxicity Study

The proposed DN alginate-pHEMA hydrogel is designed to be a coating material for medical devices such as urinary catheters and other implants; hence, it is crucial that the material is biocompatible. Although both alginate and HEMA monomers have been shown to be non-toxic and biocompatible, the crosslinking reagents and photoinitiators may be toxic, and thus, the unreacted chemicals must be removed [51, 66]. Among all of the crosslinking reagents, Irgacure 651 is the most cytotoxic and has the lowest aqueous solubility. Nevertheless, this photoinitiator is highly efficient and has been used as a crosslinker for hydrogels with bioengineering applications [67, 68]. Unlike Irgacure 651, Irgacure 2959 has been reported to exhibit significantly lower cytotoxicity than other common UV photoinitiators and is widely used in the synthesis of biomaterials [69, 70].

The SN and DN gel dishes were incubated in DMEM/F-12 medium containing 10 % fetal bovine serum and penicillin/streptomycin with HEK cells, and the resulting percentage area confluence was then compared to that of the control to determine their cytotoxicity. The photomicrographs (Figure 2.11a) show consistent growth of cell clusters in all three scenarios (SN, DN and, control). Furthermore, the cells proliferated at roughly a constant rate and reached maximum confluence (~95%) on the 6<sup>th</sup> day (Figure 2.11b), indicating that the proposed DN hydrogels did not contain cytotoxic residues after the standard wash protocol. The percentage area confluences for the SN and DN samples were noticeably larger than those of the control throughout the test, due to the different initial cell numbers in each well. Also, the larger standard errors between days 2 and 4 suggest uneven proliferation rates at different measured locations when free space was available around the cell clusters, which is considered normal for this type of assay.

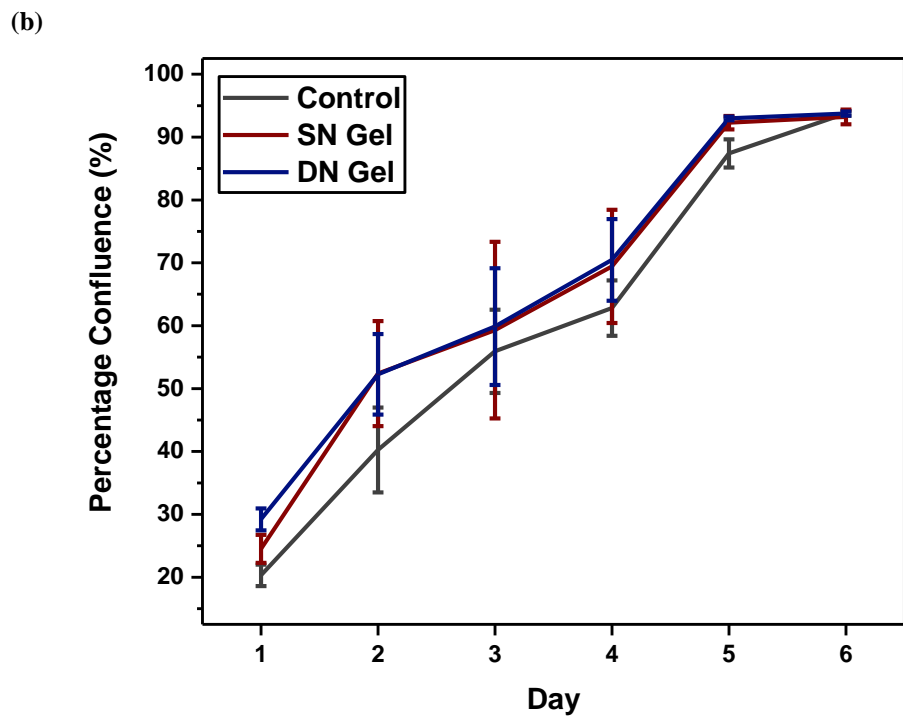
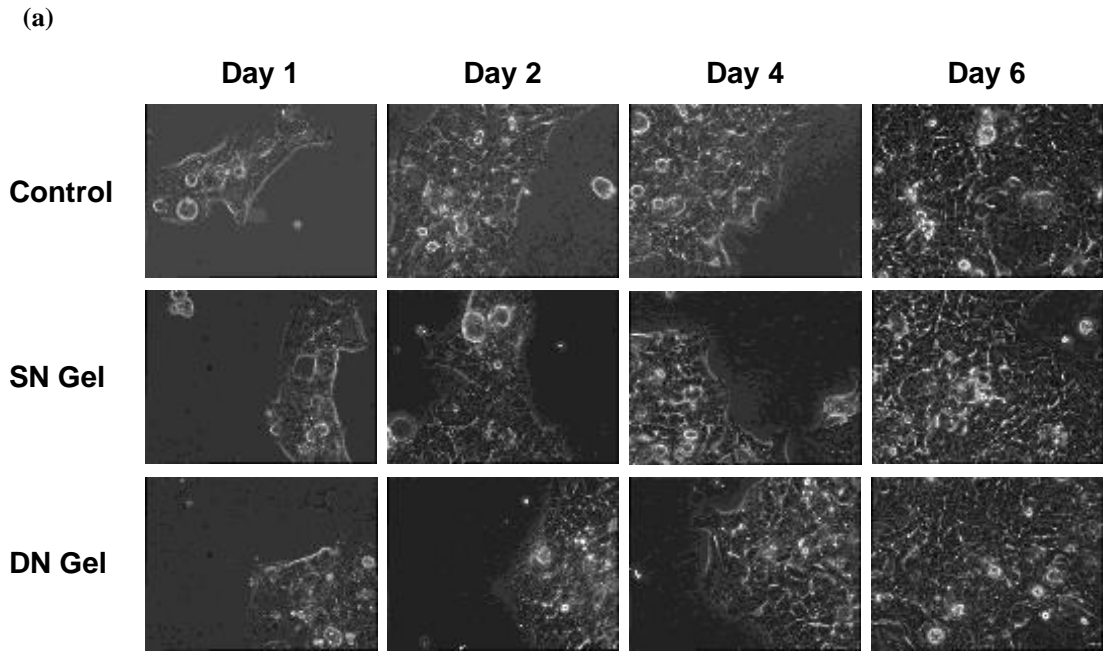


Figure 2.11 (a) OM images and (b) percentage confluence of HEK cells incubated with SN, DN gel and in control.

## Chapter 3: DN Hydrogel Coating for PDMS Devices

### 3.1 Fabrication Process

#### 3.1.1 Fabrication of PDMS Micropillar Substrates

Micropillars are incorporated on PDMS substrates to improve adhesion between the coating and the substrates [26]. Thin PDMS micropillar substrates were fabricated by a modified replica molding method, previously developed by our research group [71]. In the modified method, the master of the substrates was printed by an Asiga Pico 3D printer (Asiga USA, Anaheim, CA, USA) (Figure 3.1), instead of being made from SU-8 photoresist on a silicon wafer. Although the 3D printing method provides a convenient way for fast prototyping, the dimensions of the printed geometries were limited by the printer's pixel size. The failure rate increased dramatically with this printer when the dimensions on the XY plane fell below 100  $\mu\text{m}$ . Hence, the diameter of the each micropillar was 150  $\mu\text{m}$ , and the distance between micropillars was 350  $\mu\text{m}$ . The height of the micropillars varied, depending on the thickness of the hydrogel coating. For demonstration purposes, the height of the micropillars was set at 200  $\mu\text{m}$  for coatings that were approximately 250-350  $\mu\text{m}$  thick when cast. The detailed fabrication procedures for casting the micropillar substrates are illustrated in Appendix D.

Sylgard 184 silicone pre-elastomer and curing agent (Dow Corning Corporation, MI, USA) was mixed thoroughly at a 10:1 weight ratio and poured into a plastic mold. The pre-elastomer filled mold was placed in the de-gassing chamber for 2 h, and then, transferred to a 60°C oven. After curing for 4 h, the PDMS substrate was released from the mold and cut into the desired sizes.

### 3.1.2 Surface Modification of PDMS Micropillar Substrates

A series of chemical modification steps for the PDMS surface is shown in Figure 3.2. Step 1: the substrate was wetted with a few droplets of 70% ethyl alcohol and immersed in the  $\text{H}_2\text{O}_2:\text{HCl}:\text{H}_2\text{O}$  solution with a volume ratio of 1:1:3 for 10 min after being cleaned by air plasma (700 mTorr and 30 W) for 75 s. Step 2: the PDMS substrate was rinsed with distilled water and immersed in 5 vol-

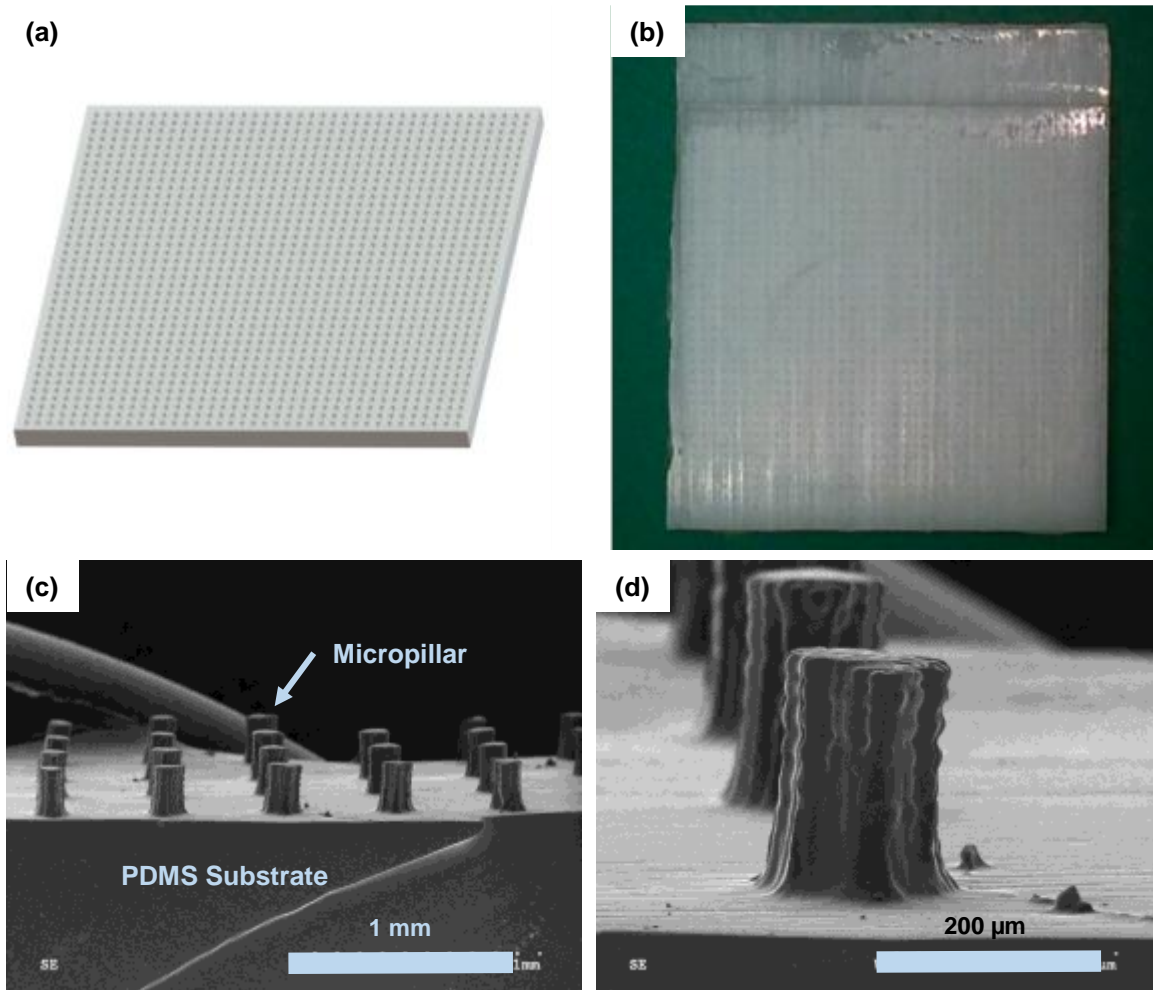


**Figure 3.1 (a) Illustration of the CAD model of 20 mm × 20 mm substrate master; (b) The plastic master printed by Asiga Pico printer; (c) SEM image of micropillar substrate; and (d) close-up of a single micropillar.**

% 3-aminopropyltriethoxysilane (APTES) solution for 60min. Finally, the substrate was rinsed again with distilled water and dried with N<sub>2</sub>.

### 3.1.3 SN Alginate Hydrogel Coating Formation

1.5 wt-% sodium alginate salt pre-gel solution (pH 5.0 in 100 mM MES buffer) was mixed with EDC, NHS and was covalently cross-linked with AAD (molar ratio of alginate: EDC:NHS:AAD = 4:6:3:1) on the APTES-treated PDMS micropillar substrate [46]. EDC was added first, and NHS was added 8 min later. AAD was added 6 min after NHS. The mixture was agitated for 30 s on a water mixer after each ingredient was added. Before the pre-gel mixture was transferred to the PDMS substrate, it was further agitated in a sonicated bath for 30 s. A PDMS-coated glass

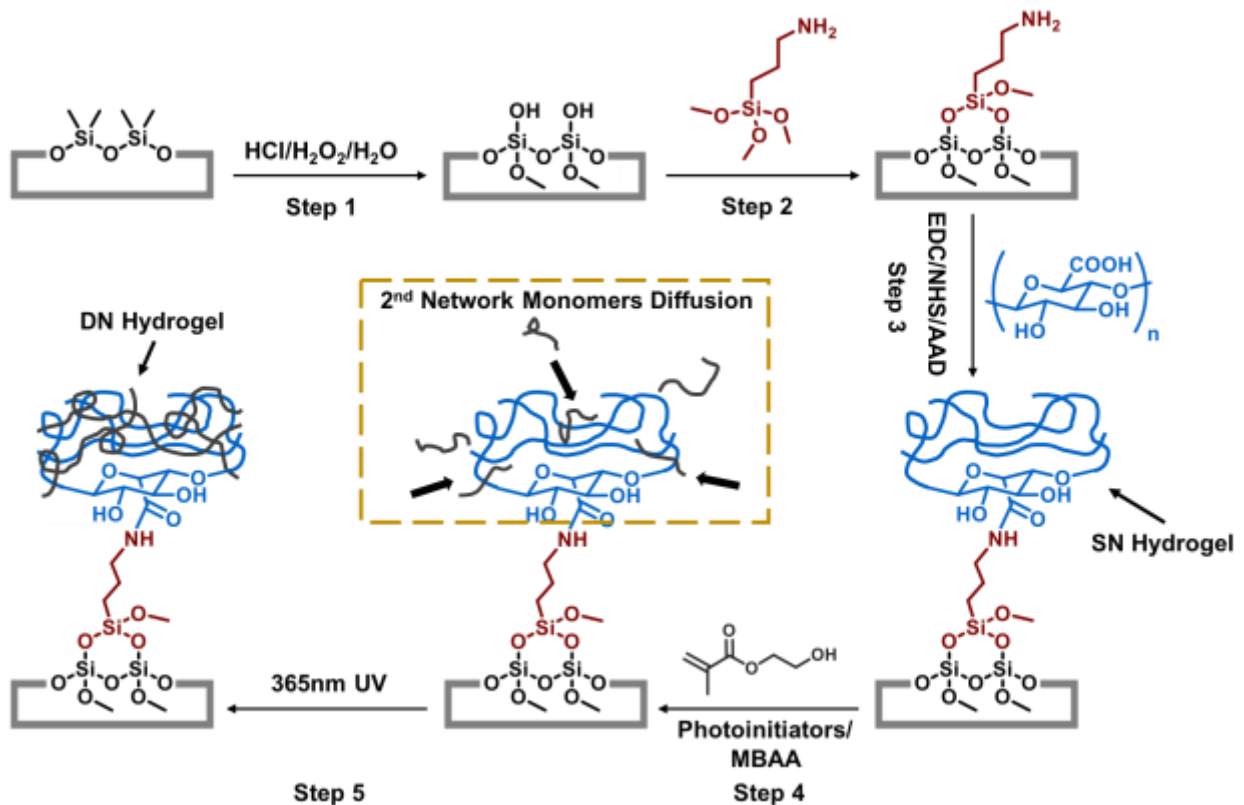


Figure 3.2 Chemical modification on PDMS substrate and DN hydrogel coating formation.

coverslip was placed on top of the pre-gel mixture with spacers (~0.5 mm) to form a thin layer of alginate hydrogel with flat surface as shown in Figure 3.2 (Step 3) and Figure 3.3. After four hours of incubation at room temperature, the entire setup was immersed in distilled water for 30 s, and then the glass coverslip was lifted from one side to prevent fracture of the alginate hydrogel.

### 3.1.4 DN Alginate-pHEMA Hydrogel Coating Formation

2 M 2-hydroxyethyl methacrylate (HEMA) was prepared in 10% ethyl alcohol containing 2.5mol% cross-linker N,N'-methylenebis(acrylamide) (MBAA), 0.5 wt-% 2,2-dimethoxy-2-phenylacetophenone (Irgacure 651), and 1 wt-% 2-hydroxy-4'-(2-hydroxyethoxy)-2-methylpropiophenone (Irgacure 2959).

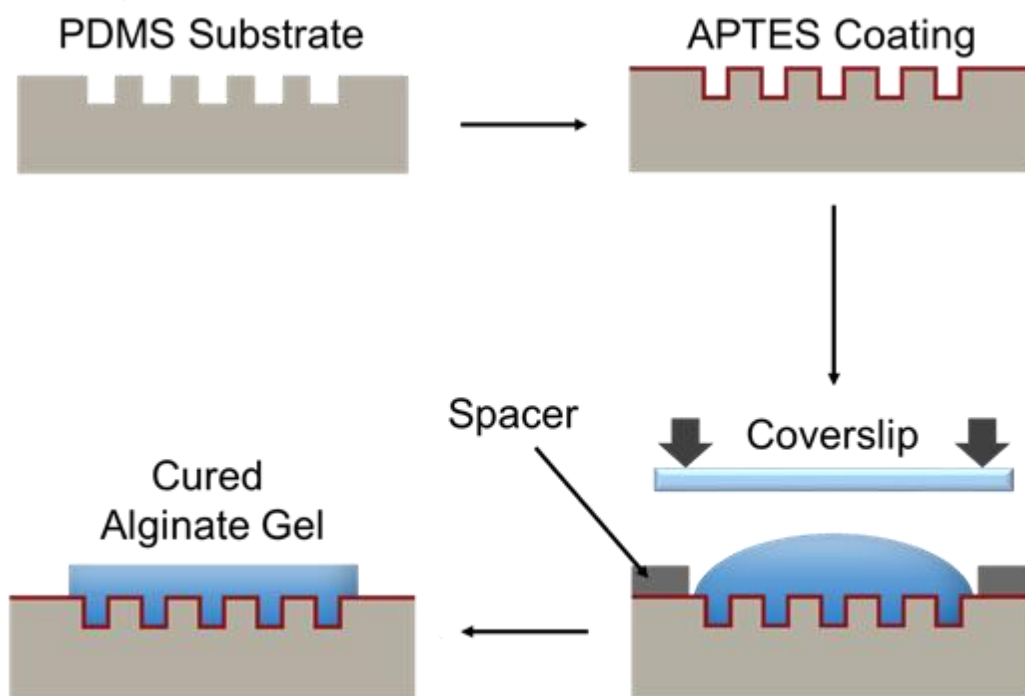
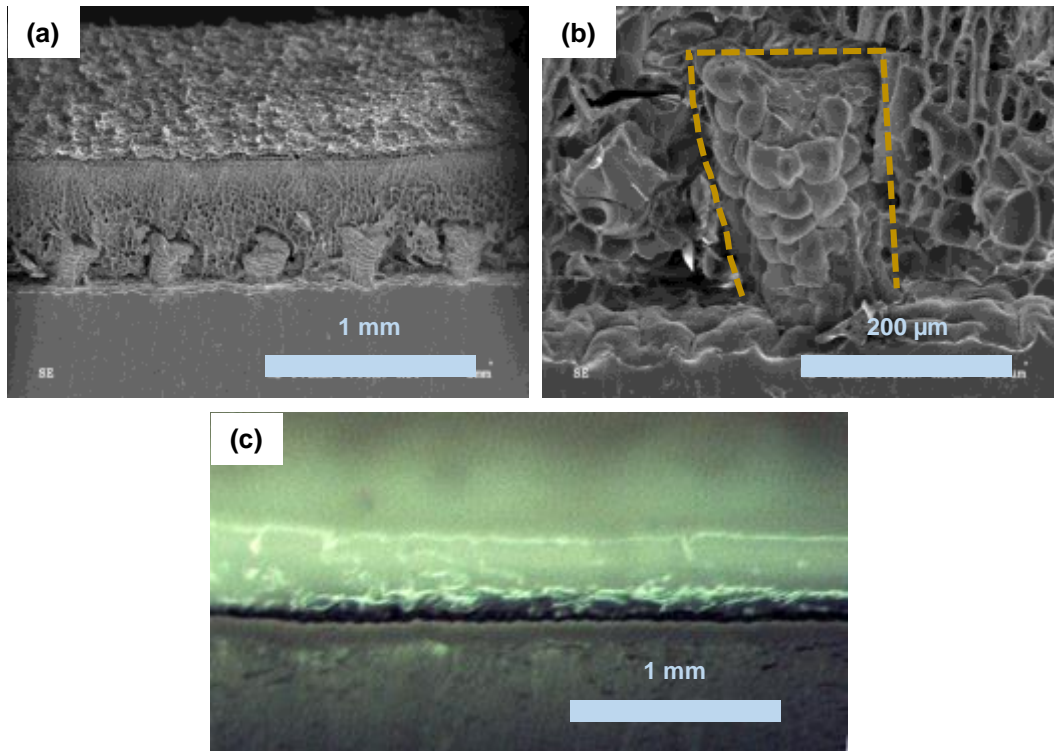


Figure 3.3 DN hydrogel coating procedures.

After 24 h of immersion in the HEMA pre-gel solution at room temperature, the alginate-coated PDMS micropillar substrate was exposed to 365 nm UV light for 20 min to form the second network of polyHEMA within the alginate network, as shown in Steps 4 and Step 5 of Figure 3.2. The resulting coated substrate was cut in half and inspected by both SEM and OM (Figure 3.4).

To



**Figure 3.4 SEM and OM images of the cross-sections of DN gel coating on micropillar substrates.**

prevent evaporation and the degradation of photoinitiators, the container holding the substrate and HEMA pre-gel solution was sealed by parafilm and wrapped with aluminum foil during the immersion process. The DN gel on the substrate was washed with 70% ethyl alcohol and DI water and then soaked in PBS solution for 36 h at room temperature.

## **3.2 Characterizations**

### **3.2.1 Detecting APTES**

An FT-IR spectrometer was used to detect APTES on the modified PDMS substrates. Both bare PDMS, OH-PDMS (intermediate product after hydrochloric acid/hydrogen peroxide treatment) and APTES-PDMS sheets were cut into 10 mm × 10 mm squares for this test; the scan number and resolution was set to 24 and 1 wavenumber, respectively.

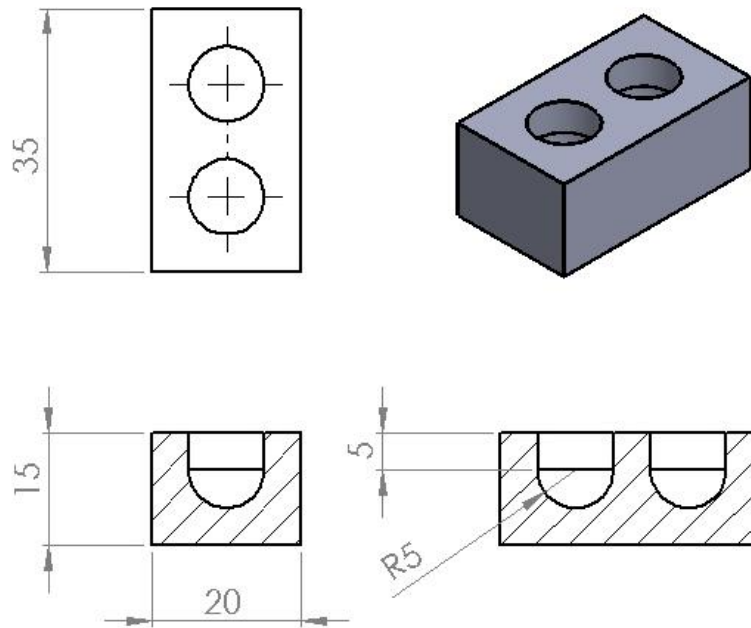
### **3.2.2 Friction Coefficient Measurement**

The friction coefficients of bare PDMS, lubricated PDMS and DN hydrogel surface were measured by Nanovea T50 (Nanovea, Irvine, CA, USA) using pin-on-disk mode with a dome-shaped PDMS test pin (radius = 10 mm, height = 10 mm). To fabricate the test pin, Sylgard 184 silicone pre-elastomer and curing agent (Dow Corning Corporation, MI, USA) were mixed thoroughly at 10:1 and poured into a plastic mold printed by an Asiga Pico 3D printer (Asiga USA, Anaheim, CA, USA) (Figure 3.5).

Separately, 50 mm × 35 mm × 1 mm glass slides were washed with 1M NaOH solution, dried with N<sub>2</sub> gas, and then cleaned with air plasma (700 mTorr and 30 W) for 75 s. To fabricate the PDMS surface, a mixture of PDMS pre-elastomer and curing agent (10:1 weight ratio) was spin-coated onto the slides at 1500 RPM for 60 s, and then the slides were incubated in a 60°C oven for 4 h. For the DN hydrogel surface, slides were treated with a H<sub>2</sub>O<sub>2</sub>/HCl/H<sub>2</sub>O mixture and 5 vol-% APTES, as described in Section 3.1.2, and a thin layer of DN hydrogel was coated onto the slides using the methods described in Sections 3.1.3 and 3.1.4.

The travel speed of the test probe was set to 5 mm/min, and the radius of its circular travel path was set to 11 mm. To avoid damaging the hydrogel coating, the normal force of all tests was limited to 1 N. The lubricated PDMS test was conducted after the bare PDMS test, using the same coated substrates, but a thin layer of K-Y Jelly was applied onto the coating prior to the new test.

(a)



(b)

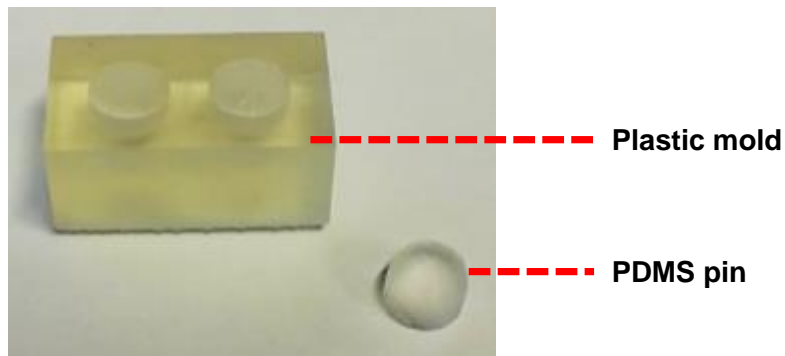


**Figure 3.5 (a) The schematic and dimensions of the printed plastic mold for PDMS test pin (unit: mm) and (b) a printed plastic mold and cured PDMS test pin cast from the mold.**

### **3.2.3 Contact Angle Measurement**

Water contact angles on bare PDMS, lubricated PDMS, and DN hydrogel surface were investigated. The samples were placed on a platform between a flashlight and a microscope; all three were adjusted to the same height. The flashlight was covered with a piece of paper to achieve a softer ambient light.

For the bare and the lubricated PDMS test, a large PDMS sheet (approximately 2 mm thick) was cut into 15 mm × 10 mm pieces, on which 4  $\mu$ l distilled water droplets were placed. Separately, the DN hydrogel coating (0.25-0.35 mm thick when cast) was cast onto a piece of 20 mm × 30 mm APTES-coated glass slide, and the contact angles of the 4  $\mu$ l distilled water droplets were measured at different locations of the single sample. Importantly, lab tissue was used to use lab tissue to absorb all excessive water on the hydrogel coating surface prior to the release of water droplets.

### **3.2.4 Evaluation of Hydrogel-PDMS Bonding Strength**

The adhesion strength between alginate-pHEMA double-network hydrogel and chemically modified PDMS (with and without micropillars) was evaluated by comparing the force required to separate a pair of chemically modified PDMS substrates, bonded together with alginate-pHEMA hydrogel, in a uniaxial direction [72]. The master for the micropillar PDMS substrates (Appendix A) was printed using an Asiga Pico 3D printer (Asiga USA, Anaheim, CA, USA), and the final substrates were fabricated with Sylgard 184 silicone pre-elastomer and curing agent at a 10:1 weight ratio (Dow Corning Corporation, MI, USA), with a replica molding method [71]. The bare PDMS substrates (2.5 cm × 1 cm × ~1.5 mm) were cut from a piece of Sylgard 184 silicone sheet.

Both micropillar and bare PDMS substrates were chemically modified using the method described in Section 3.1.2.

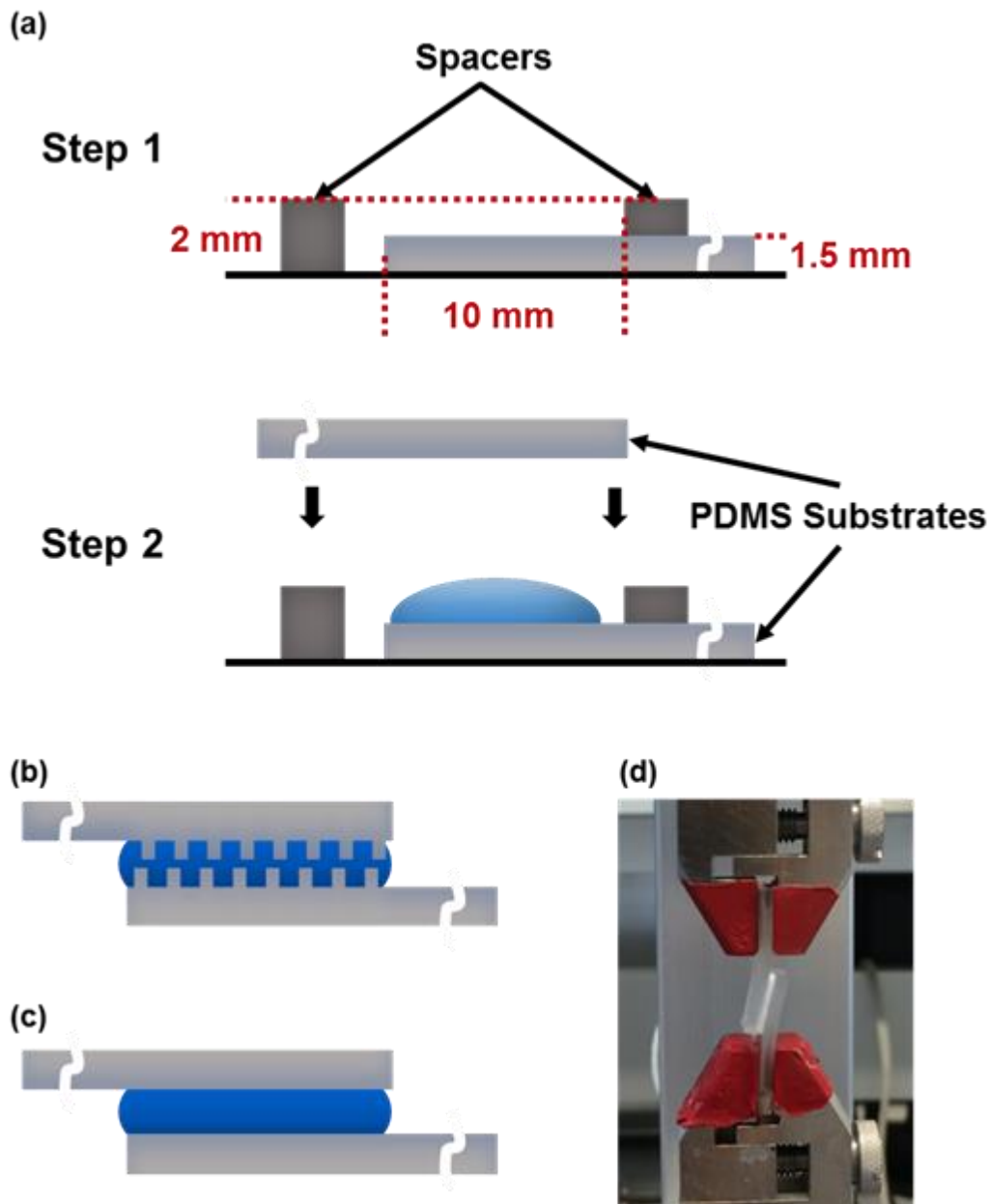


**Figure 3.6 (a) Fabrication process for the lap-shear test strips, (b) the cross-section view of test ribbon with micropillars, (c) the cross-section view of test ribbon without micropillars, and (d) experiment setup.**

SN alginate gel (molar ratio of alginate:EDC:NHS:AAD = 4:6:3:1) was assembled between two chemically modified PDMS strips with a square overlapping area of 1 cm<sup>2</sup>. Figure 3.6a shows the two-step assembly process. Step 1: a 0.5 mm-thick ABS plastic plate was used as the spacer on the right, and the left spacer was made from the same ABS plastic plate stacked on a piece of PDMS (same thickness as the bottom substrate). Step 2: approximately 60  $\mu$ l pre-gel solution was placed on the target area of the bottom substrate. Then, the top PDMS substrate was stacked onto the spacer and aligned with the bottom substrate. The top substrate was gently pressed to ensure that the pre-gel solution covered the entire overlapping region; however, the force was not large enough to deform the top substrate. Figures 3.6b and 3.6c show the cross-sectional view of the composites with and without micropillars, respectively. The composite was then immersed in 2 M HEMA monomer solution for 48 hours prior to exposure to 365 nm UV light for 20 min, and it was then immersed in PBS solution for 24 h. The PDMS was then clamped onto a Bose Electroforce BioDynamic 5100 tester (Bose, USA) (Figure 3.6d), and were continuously stretched at a rate of 0.167 mm/s until they were detached from each other.

### **3.3 Results and Discussion**

#### **3.3.1 Chemical Modification on PDMS Substrates**

Due to the discrepancy between the hydrophilicity of PDMS and hydrogels, a major challenge is in achieving stable adhesion between the two materials. To overcome the challenge, chemical modification on PDMS surfaces has been introduced. Molecules, such as APTES and TMSPPMA, are attached to the PDMS surface and covalently linked to hydrogel to allow permanent adhesion of hydrogel onto the PDMS. To attach the bonding agents to the PDMS surface, the surface must be oxidized by HCl and H<sub>2</sub>O<sub>2</sub> first to replace oxygen atoms with hydroxyl groups (Figure 3.2: step

1), and then, the ethoxy groups on the APTES or TMSPMA couples with the hydroxyl groups on the PDMS surface (Figure 3.2: step 2). APTE is used as the bonding agent in this project since alginate is the first network of the proposed coating; the conjugation is attained through carbodiimide-amide coupling between amidogen groups on ATPES and carboxyl groups of alginate monomers (Figure 3.2: step 3) [25, 26].

Since cosmetic change was not observed during these processes, the efficiency of chemical modification was confirmed with FT-IR spectroscopy. As shown in Figure 3.7, a peak at  $3366\text{ cm}^{-1}$  represents carboxyl groups on the PDMS surface, and the formation of OH-PDMS [73].

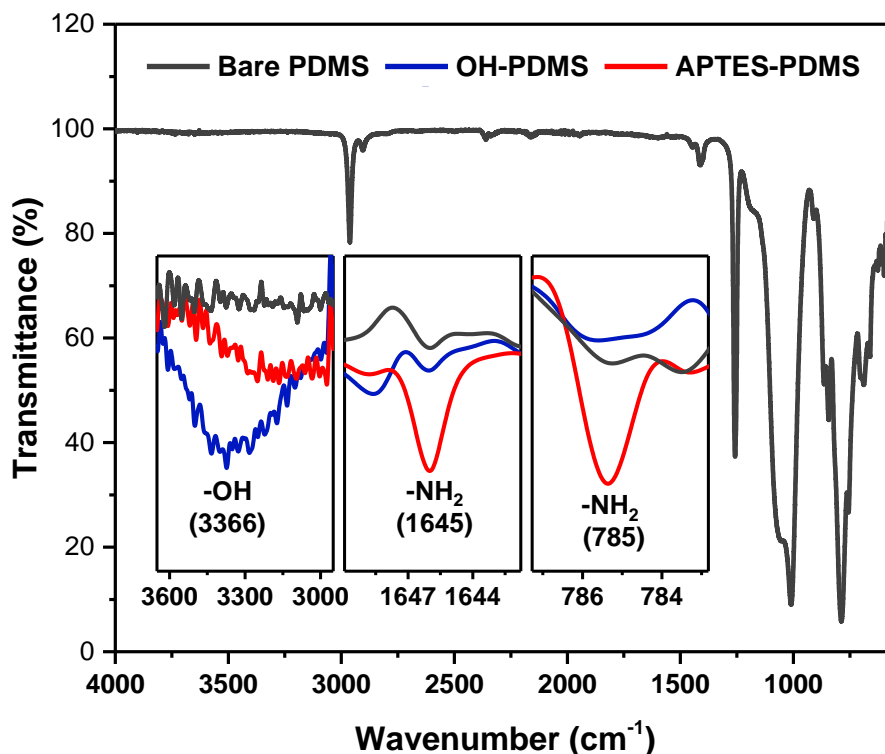


Figure 3.7 FT-IR spectroscopy of bare PDMS, OH-PDMS and APTES-PDMS.

Carboxyl groups were consumed after OH-PDMS was treated with APTES, which explains the disappearance of the peak at  $3366\text{ cm}^{-1}$ . The FT-IR transmittance peak at  $1645\text{ cm}^{-1}$  represents  $\text{NH}_2$  scissoring, and the peak at  $785\text{ cm}^{-1}$  represents  $\text{NH}_2$  wagging and twisting; both signals result from amidogen groups of APTES attached to the PDMS surface. We used the scan of bare PDMS as the background to generate the transmittance spectrum for APTES-coated PDMS.

### **3.3.2 Adhesion Strength between Coating and Substrate**

In addition to the aforementioned chemical modification on PDMS substrates, micropillars were also incorporated to improve coating stability. Not only can the micropillars act as anchors to restrain the potential movement of the coating, but they also increase the contact area between the gel solution and the PDMS substrate, leading to an increased number of covalent bonds between the substrate and alginate chains. As expected, the micropillar PDMS substrate bonded to the DN alginate-pHEMA hydrogel more securely, in comparison to its bare counterpart; the improvement was approximately 54.9% for the current micropillar design (Figure 3.8a). Moreover, the SEM and OM images show significant amount of hydrogel residue left on the bonding sites after micropillar PDMS strips were pulled apart, indicating that failure was due to the fracture of the DN hydrogel itself (Figure 3.8b). The DN hydrogel layer on the bare PDMS strips, in contrast, remained intact and sheared off from one substrate cleanly after the test, indicating that the failure occurred at the bonding site (Figure 3.8c); however, during the fabrication of test strips, we noticed that chemical modification dramatically improved the wettability of the PDMS surface, causing the pre-gel solution to more easily spread across the bonding area. The adhesion strength between unmodified substrates (bare or micropillar) and the hydrogel coating could not be tested as the two materials often detached from each other during the fabrication processes. The results indicate that

chemical modification is necessary to create a stable hydrogel coating on the PDMS substrate, and micropillar anchors can be used to further improve the bonding strength between two the materials.

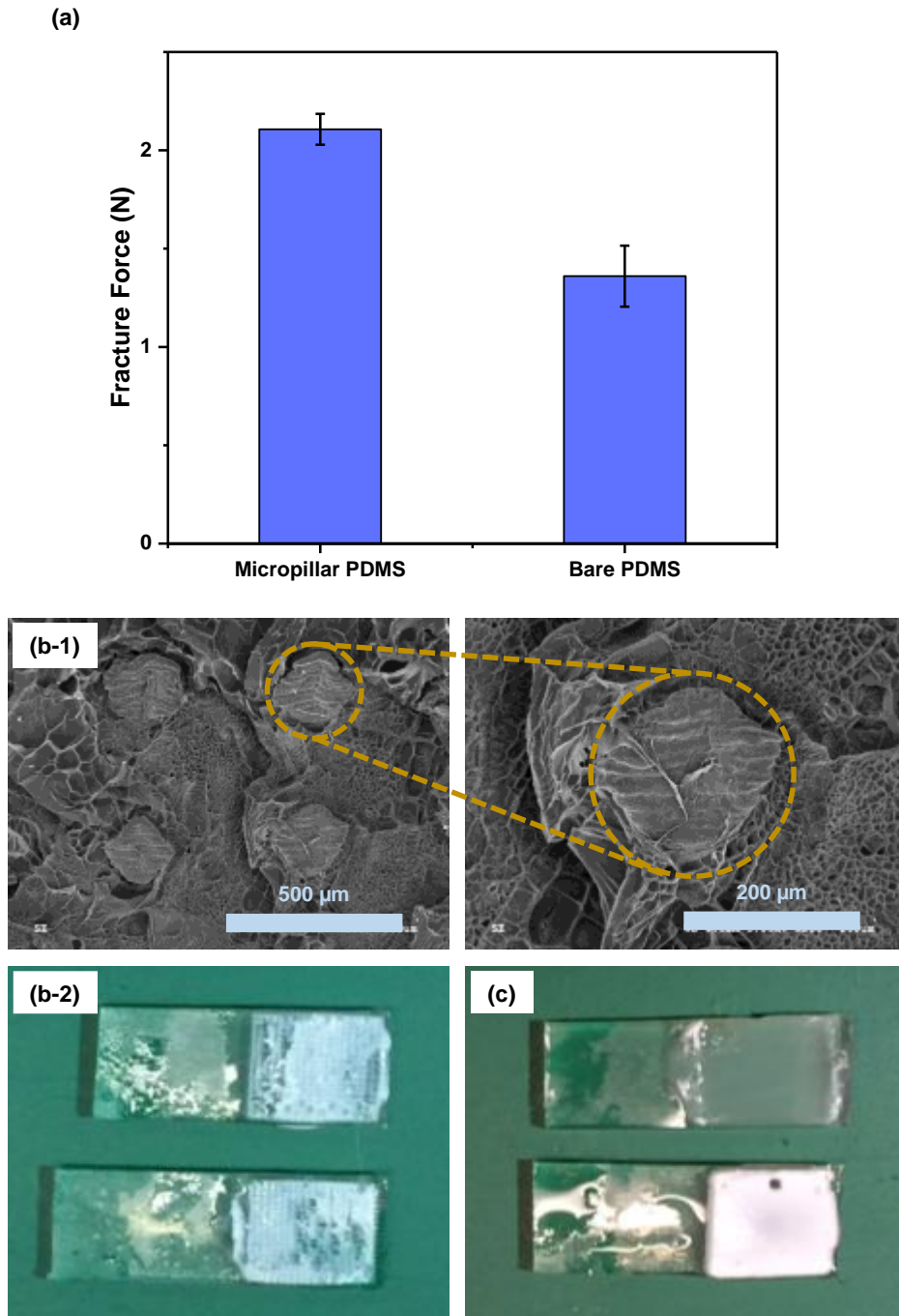


**Figure 3.8 (a) Maximal force to separate the bonded strips, (b) separated micropillar strips and (c) separated bare PDMS strips.**

Only one pillar design was tested since investigating the correlation between micropillar designs and bonding strength was not the primary purpose of this project. Because of the complex geometry at the bonding site, the bonding strength was compared using the fracture force, instead of adhesion energy [72].

### **3.3.3 Wettability and Friction Coefficient of Gel-coated Surface**

Wettability of bare PDMS, lubricated PDMS, and hydrogel-coated PDMS substrates were evaluated by comparing the water contact angles on these surfaces (Figure 3.9a). Bare PDMS exhibited the highest hydrophobicity with a contact angle of  $106\pm 0.84^\circ$  (Figure 3.9b). A thin layer of K-Y Jelly reduced this value to  $44.68\pm 1.57^\circ$  (Figure 3.9b), indicating an improved wettability on PDMS substrates; however, this layer of lubrication can be easily washed off by water, making it unsuitable for any medical implants. The hydrogel-coated PDMS is believed to have the highest wettability, judged by the fact that water did not form distinct droplets on the coating surface.

Our study of the surface friction showed that the hydrogel-coated PDMS had the lowest friction coefficient of  $0.07\pm 0.00$  against a PDMS pin (Figures 3.10a and 3.10b). The ultra-low friction of DN hydrogel is attributed to lubrication of the hydrated water layer, which is supplied by the body water stored in the gel network [74]. Without any modification, the bare PDMS had a significantly higher friction coefficient of  $0.50\pm 0.02$ ; and even with traditional lubrication (e.g., K-Y Jelly), the friction coefficient was still nearly three-fold higher than that of the hydrogel-coated PDMS (Figure 3.10b). For biomedical applications such as silicone urinary catheters, having an ultra-low surface friction is crucial to decrease the discomfort during catheterization. While traditional lubrication is only available during the catheter's insertion, and it will disperse over time; the

hydrogel coating is a more durable alternative to retain minimal surface friction during both insertion and removal.

The incorporation of the proposed DN hydrogel coating drastically lowers the surface friction of PDMS-based implants, minimizing the use of lubrication and reducing the insertion difficulty. The enhanced hydrophilicity might reduce the adhesion of unwanted biomolecules onto PDMS-based

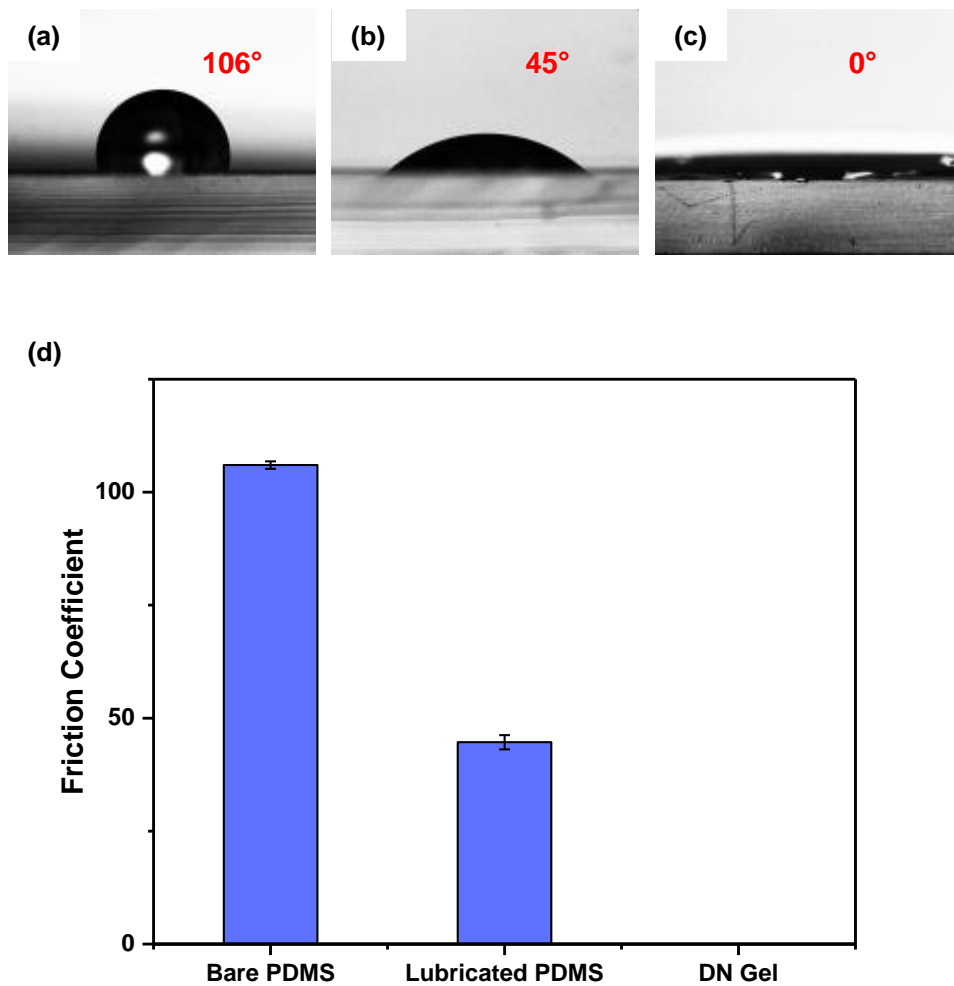


**Figure 3.9** Water droplets on (a) bare PDMS, (b) lubricated PDMS and (c) DN hydrogel surface, and (d) the contact angles of water on these surfaces.

medical devices and make introducing aqueous solutions into PDMS micro-channels easier, which would greatly benefit surgical implants and analytical devices [8, 17].

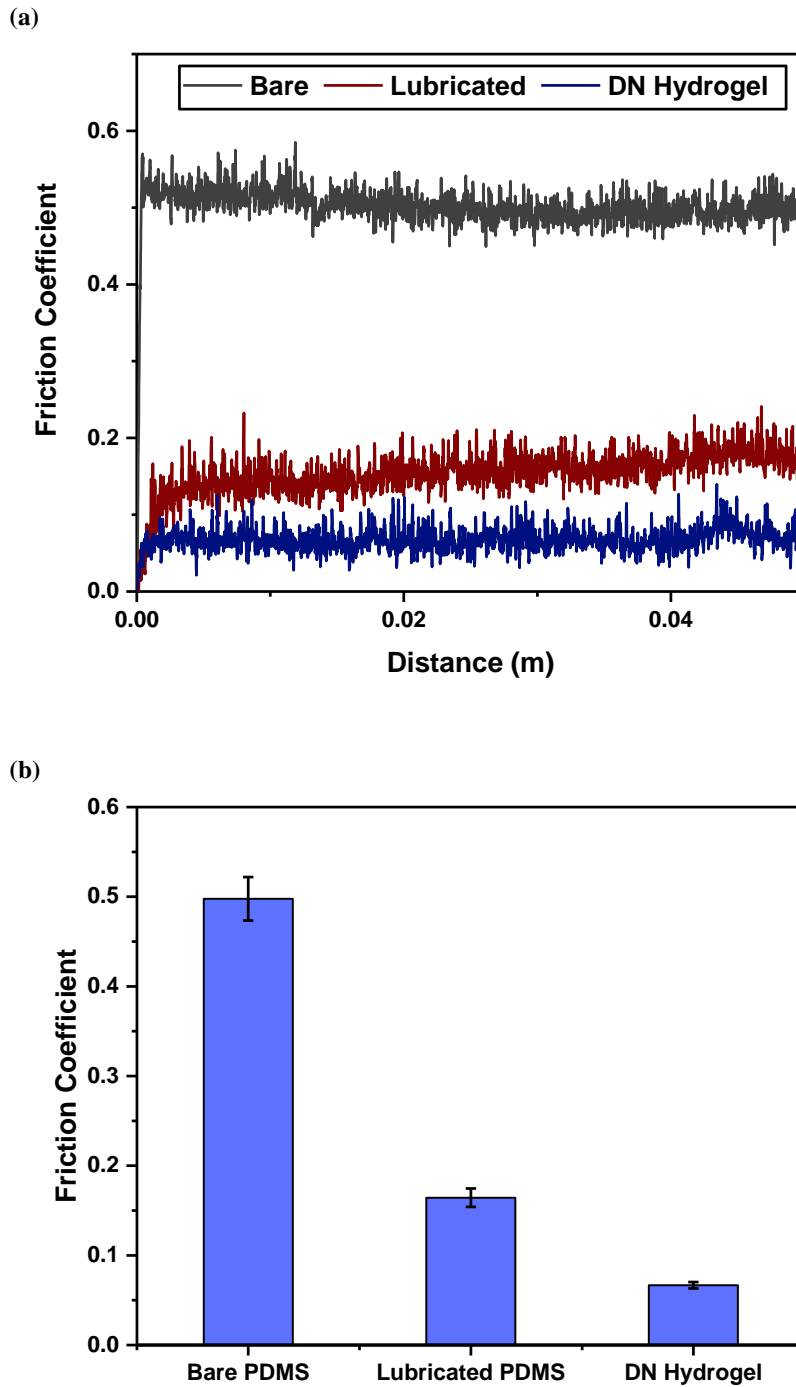


Figure 3.10 (a) Friction coefficient of various substrates and (b) their comparison.

## **Chapter 4: Conclusion**

The introductory chapter in this thesis had a literature review on surface modifications for PDMS-based biomedical implants. The second chapter described the design, fabrication, and characterizations of the DN alginate-pHEMA hydrogel, with a discussion of results. In Chapter 3, the design and modification of micropillar substrates, coating formation processes, characterizations of coated and native PDMS, and a discussion of results was presented. The final chapter summarizes the work done in this project, highlights the significance of the proposed DN gel coating, and suggests directions for future research.

### **4.1 Summary**

Chapter 1 briefly reviewed the disadvantages of widely used PDMS-based biomedical implants, such as silicone urinary catheters, and the existing surface modification techniques that are used to overcome these challenges. The techniques were classified into two types: energy treatment and polymer coatings. Numerous coating methods were reviewed and categorized as Teflon coatings, radiation-induced graft for hydrogels, and chemical modifications for hydrogels. Some potential hydrogel candidates were presented, with their pros and cons. Finally, a double-network hydrogel coating, based on an alginate and pHEMA hydrogel was proposed.

In Chapter 2, the double-network structure and the crosslinking mechanisms of alginate and pHEMA hydrogel were explained. Although the alginate gel could be ionically and covalently crosslinked, we chose covalent crosslinking techniques, because of their stability in biological environments and their ease of fabrication [25, 55, 56]. Because the monomer size of alginate is

hundreds of times larger than that of HEMA, the pore size of an alginate network is also considerably larger, creating a nest structure (Figure 2.9).

The influence of the pHEMA network density on the mechanical properties of DN gel was investigated via trial and error method. Several HEMA monomer and crosslinker combinations were tested in a two-step process. 2 M HEMA monomers and 2.5 mol-% crosslinker MBAA was chosen as the final formulation for this project. Although it had a lower fracture stress of  $502.04 \pm 14.41$  kPa, its Young's modulus of  $28.86 \pm 1.78$  kPa was a better mimic of urethral tissue. This was not the optimal formulation; however, since material optimization was not the objective of this project.

The double-network structure introduced a denser pHEMA network within the pores of the alginate hydrogel, significantly reducing the swelling of gels in PBS solution. On the other hand, the presence of the pHEMA network also lowered the equilibrium water content of the hydrogels. Neither the SN alginate gel nor the DN alginate-pHEMA gel exhibited any cytotoxicity in the cytotoxicity study. The percentage area confluence of the SN and DN gels reached their maximums at the same time as that of the control.

Chapter 3 began with the section covering the design, fabrication of the micropillar PDMS substrates and chemical modification methods of the substrate. The modified PDMS was examined by FT-IR spectroscopy, and the  $-OH$  groups after oxidation and  $-NH_2$  groups after APTES treatment were observed.

The hydrogel-substrate bonding strength was evaluated in a shear test, where two APTES-PDMS ribbons were glued together by the DN alginate-pHEMA hydrogel and pulled apart by a tensile

tester. The ribbons with micropillars were roughly 55% stronger than those without micropillars and they broke at  $2.11 \pm 0.08$  N of force. Then, the morphology of the binding area was investigated and the SEM images showed a large amount of hydrogel residues on the binding areas after the fracture, indicating that the fracture was primarily caused by material failure not because of adhesion strength.

The proposed hydrogel coating successfully reduced the friction coefficient from  $0.50 \pm 0.02$  of native PDMS to  $0.07 \pm 0.00$ . The hydrogel coating was more long-lasting and performed considerably better in terms of friction reduction than K-Y Jelly lubricant. The substrates that were coated with hydrogel also exhibited superior hydrophilicity; the water contact angle on the hydrogel coating was approximately  $0^\circ$ , in comparison to  $106.00 \pm 0.84^\circ$  on bare PDMS substrates.

## **4.2 Future Work**

One direction for future work is to optimize the mechanical properties of the DN hydrogel coating. The strength of the material itself could be improved by adjusting the monomer and crosslinker contents for both the first and the second networks. The DN hydrogel's anti-fouling properties could also be improved by incorporating new materials, such as PEG and Zwitterionic hydrogels, into the second network [41]. Adhesion strength is correlated to substrate surface morphology and the number of  $-\text{NH}_2$  functional groups. Different micropillar designs or completely new surface texture, like porous surfaces, could be tested. Moreover, the concentration of APTES solutions are well known to affect the number of functional groups; hence, a thorough study on optimized APTES solutions could be useful [25].

Another direction is to explore the fabrication techniques. Currently, the DN hydrogel coating is cast on a flat PDMS substrate for demonstration purposes. A simple and efficient method is needed to coat hydrogel onto tubular implants (e.g., urinary catheters or cardiac catheters). Commercially available catheters without micropillars could be used for the sole purpose of studying the coating methods. To create even coatings with the desired thickness, the molding method would be preferred, where chemically modified catheters, reinforced with rigid stents, are pushed through a cylindrical mold filled with pre-gel solution. The excess pre-gel solution would be displaced, leaving enough pre-gel solution in the gap between the catheter and the mold.

Finally, antibiotic drugs or silver nanoparticles could be loaded into hydrogel coating to tackle infection. Drugs can be released from gel networks in a controlled manner, with the release rate depending on crosslinker types and crosslinking methods [44]. Agar diffusion tests could be used to study antibacterial performance and effective times for the loaded drugs. Another approach is to embed silver nanoparticles in the hydrogel coating. The nanoparticles can be synthesized via chemical reduction of silver nitrate solution [75]. This work should also consider the correlation between nanoparticle size and antibacterial performance.

## References

- [1] P. N. Eleni, I. Katsavou, M. K. Krokida, G. L. Polyzois, and L. Gettleman, "Mechanical behavior of facial prosthetic elastomers after outdoor weathering," *Dent Mater*, vol. 25, pp. 1493-502, Dec. 2009.
- [2] J. H. Park, K. B. Lee, I. C. Kwon, and Y. H. Bae, "PDMS-based polyurethanes with MPEG grafts: Mechanical properties, bacterial repellency, and release behavior of rifampicin," *Journal of Biomaterials Science, Polymer Edition*, vol. 12, pp. 629-645, 2001.
- [3] L. Liu and H. Sheardown, "Glucose permeable poly (dimethyl siloxane) poly (N-isopropyl acrylamide) interpenetrating networks as ophthalmic biomaterials," *Biomaterials*, vol. 26, pp. 233-44, Jan. 2005.
- [4] M. C. Bélanger and Y. Marois, "Hemocompatibility, biocompatibility, inflammatory and in vivo studies of primary reference materials low-density polyethylene and polydimethylsiloxane: A review," *Journal of Biomedical Materials Research*, vol. 58, pp. 467-477, 2001.
- [5] J. C. McDonald and G. M. Whitesides, "Poly(dimethylsiloxane) as a Material for Fabricating Microfluidic Devices," *Accounts of Chemical Research*, vol. 35, pp. 491-499, Jul. 1, 2002.
- [6] F. N. Pirmoradi, J. K. Jackson, H. M. Burt, and M. Chiao, "A magnetically controlled MEMS device for drug delivery: design, fabrication, and testing," *Lab Chip*, vol. 11, pp. 3072-80, Sep. 21, 2011.
- [7] A. Khademhosseini, R. Langer, J. Borenstein, and J. P. Vacanti, "Microscale technologies for tissue engineering and biology," *Proceedings of the National Academy of Sciences of*

- the United States of America*, vol. 103, pp. 2480-2487, Feb. 13, 2006.
- [8] H. Makamba, J. H. Kim, K. Lim, N. Park, and J. H. Hahn, "Surface modification of poly(dimethylsiloxane) microchannels," *Electrophoresis*, vol. 24, pp. 3607-19, Nov. 2003.
- [9] L. Liu, B. Ercan, and T. Webster, "Decreased Bacterial Activity on Nano-patterned PDMS Replica for Catheter-associated Infection Prevention," *The FASEB Journal*, vol. 29, p. LB649, 2015.
- [10] A. J. C. Cox, D. W. L. Hukins, and T. M. Sutton, "Infection of catheterised patients: bacterial colonisation of encrusted Foley catheters shown by scanning electron microscopy," *Urological Research*, vol. 17, pp. 349-352, Nov. 1989.
- [11] B. Foxman, "The epidemiology of urinary tract infection," *Nat Rev Urol*, vol. 7, pp. 653-60, Dec. 2010.
- [12] W. E. Stamm, "Catheter-associated urinary tract infections: Epidemiology, pathogenesis, and prevention," *The American Journal of Medicine*, vol. 91, pp. S65-S71, Sep. 16, 1991.
- [13] C. V. Gould, C. A. Umscheid, R. K. Agarwal, G. Kuntz, D. A. Pegues, and C. Healthcare Infection Control Practices Advisory, "Guideline for prevention of catheter-associated urinary tract infections 2009," *Infect Control Hosp Epidemiol*, vol. 31, pp. 319-26, Apr. 2010.
- [14] P. Tanabe, "Factors Affecting Pain Scores during Female Urethral Catheterization," *Academic Emergency Medicine*, vol. 11, pp. 699-702, 2004.
- [15] Y. Uyama, H. Tadokoro, and Y. Ikada, "Low-frictional catheter materials by photo-induced graft polymerization," *Biomaterials*, vol. 12, pp. 71-75, Jan. 1991.
- [16] C. Chung, M. Chu, R. Paoloni, M. J. O'Brien, and T. Demel, "Comparison of lignocaine and water-based lubricating gels for female urethral catheterization: a randomized

- controlled trial," *Emerg Med Australas*, vol. 19, pp. 315-9, Aug. 2007.
- [17] J. Zhou, A. V. Ellis, and N. H. Voelcker, "Recent developments in PDMS surface modification for microfluidic devices," *Electrophoresis*, vol. 31, pp. 2-16, Jan. 2010.
- [18] K. Efimenko, W. E. Wallace, and J. Genzer, "Surface Modification of Sylgard-184 Poly(dimethyl siloxane) Networks by Ultraviolet and Ultraviolet/Ozone Treatment," *Journal of Colloid and Interface Science*, vol. 254, pp. 306-315, 2002.
- [19] E. L. Lawrence and I. G. Turner, "Materials for urinary catheters: a review of their history and development in the UK," *Med Eng Phys*, vol. 27, pp. 443-53, Jul. 2005.
- [20] D. Graiver, R. L. Durall, and T. Okada, "Surface morphology and friction coefficient of various types of Foley catheter," *Biomaterials*, vol. 14, pp. 465-469, May. 1993.
- [21] D. Bodas and C. Khan-Malek, "Hydrophilization and hydrophobic recovery of PDMS by oxygen plasma and chemical treatment—An SEM investigation," *Sensors and Actuators B: Chemical*, vol. 123, pp. 368-373, 2007.
- [22] X. Ren, M. Bachman, C. Sims, G. P. Li, and N. Allbritton, "Electroosmotic properties of microfluidic channels composed of poly(dimethylsiloxane)," *Journal of Chromatography B: Biomedical Sciences and Applications*, vol. 762, pp. 117-125, Oct. 25, 2001.
- [23] Y. H. An and R. J. Friedman, "Concise review of mechanisms of bacterial adhesion to biomaterial surfaces," *Journal of Biomedical Materials Research*, vol. 43, pp. 338-348, 1998.
- [24] M. Talja, M. Ruutu, L. C. Andersson, and O. Alfthan, "Urinary catheter structure and testing methods in relation to tissue toxicity," *Br J Urol*, vol. 58, pp. 443-9, Aug. 1986.
- [25] C. Cha, E. Antoniadou, M. Lee, J. H. Jeong, W. W. Ahmed, T. A. Saif, *et al.*, "Tailoring hydrogel adhesion to polydimethylsiloxane substrates using polysaccharide glue," *Angew*

- Chem Int Ed Engl*, vol. 52, pp. 6949-52, Jul. 1, 2013.
- [26] H. Zhang, C. Bian, J. K. Jackson, F. Khademolhosseini, H. M. Burt, and M. Chiao, "Fabrication of robust hydrogel coatings on polydimethylsiloxane substrates using micropillar anchor structures with chemical surface modification," *ACS Appl Mater Interfaces*, vol. 6, pp. 9126-33, Jun. 25, 2014.
- [27] A. Mata, A. J. Fleischman, and S. Roy, "Characterization of Polydimethylsiloxane (PDMS) Properties for Biomedical Micro/Nanosystems," *Biomedical Microdevices*, vol. 7, pp. 281-293, 2005.
- [28] H. Hillborg, J. F. Ankner, U. W. Gedde, G. D. Smith, H. K. Yasuda, and K. Wikström, "Crosslinked polydimethylsiloxane exposed to oxygen plasma studied by neutron reflectometry and other surface specific techniques," *Polymer*, vol. 41, pp. 6851-6863, Aug. 2000.
- [29] J. A. Vickers, M. M. Caulum, and C. S. Henry, "Generation of Hydrophilic Poly(dimethylsiloxane) for High-Performance Microchip Electrophoresis," *Analytical Chemistry*, vol. 78, pp. 7446-7452, Nov. 1, 2006.
- [30] Y. Berdichevsky, J. Khandurina, A. Guttman, and Y. H. Lo, "UV/ozone modification of poly(dimethylsiloxane) microfluidic channels," *Sensors and Actuators B: Chemical*, vol. 97, pp. 402-408, 2004.
- [31] I. E. Araci, B. Su, S. R. Quake, and Y. Mandel, "An implantable microfluidic device for self-monitoring of intraocular pressure," *Nat Med*, vol. 20, pp. 1074-8, Sep. 2014.
- [32] M. Ruutu, O. Alfthan, M. Talja, and L. C. Andersson, "Cytotoxicity of Latex Urinary Catheters," *British Journal of Urology*, vol. 57, pp. 82-87, 1985.
- [33] S. Hu, X. Ren, M. Bachman, C. E. Sims, G. P. Li, and N. Allbritton, "Surface Modification

- of Poly(dimethylsiloxane) Microfluidic Devices by Ultraviolet Polymer Grafting," *Analytical Chemistry*, vol. 74, pp. 4117-4123, Aug. 1, 2002.
- [34] S. Jiang, S. Liu, and W. Feng, "PVA hydrogel properties for biomedical application," *J Mech Behav Biomed Mater*, vol. 4, pp. 1228-33, Oct. 2011.
- [35] N. A. Peppas and N. K. Mongia, "Ultrapure poly(vinyl alcohol) hydrogels with mucoadhesive drug delivery characteristics," *European Journal of Pharmaceutics and Biopharmaceutics*, vol. 43, pp. 51-58, Jan. 1997.
- [36] C. M. Hassan and N. A. Peppas, "Structure and Applications of Poly(vinyl alcohol) Hydrogels Produced by Conventional Crosslinking or by Freezing/Thawing Methods," in *Biopolymers · PVA Hydrogels, Anionic Polymerisation Nanocomposites*, ed Berlin, Heidelberg: Springer Berlin Heidelberg, 2000, pp. 37-65.
- [37] T. Tanigami, K. Yano, K. Yamaura, and S. Matsuzawa, "Anomalous swelling of poly(vinyl alcohol) film in mixed solvents of dimethylsulfoxide and water," *Polymer*, vol. 36, pp. 2941-2946, Jan. 1995.
- [38] J. Zhu, "Bioactive modification of poly(ethylene glycol) hydrogels for tissue engineering," *Biomaterials*, vol. 31, pp. 4639-56, Jun. 2010.
- [39] M. B. Browning, T. Wilems, M. Hahn, and E. Cosgriff-Hernandez, "Compositional control of poly(ethylene glycol) hydrogel modulus independent of mesh size," *J Biomed Mater Res A*, vol. 98, pp. 268-73, Aug. 2011.
- [40] S. Krishnan, C. J. Weinman, and C. K. Ober, "Advances in polymers for anti-biofouling surfaces," *Journal of Materials Chemistry*, vol. 18, p. 3405, 2008.
- [41] H. Zhang and M. Chiao, "Anti-fouling Coatings of Poly(dimethylsiloxane) Devices for Biological and Biomedical Applications," *Journal of Medical and Biological Engineering*,

- vol. 35, pp. 143-155, 2015.
- [42] C.-D. Young, J.-R. Wu, and T.-L. Tsou, "High-strength, ultra-thin and fiber-reinforced pHEMA artificial skin," *Biomaterials*, vol. 19, pp. 1745-1752, Oct. 1998.
- [43] E. J. Castillo, J. L. Koenig, J. M. Anderson, and J. Lo, "Protein adsorption on hydrogels," *Biomaterials*, vol. 6, pp. 338-345, Sep. 1985.
- [44] K. Y. Lee and D. J. Mooney, "Alginate: properties and biomedical applications," *Prog Polym Sci*, vol. 37, pp. 106-126, Jan. 2012.
- [45] G. T. Grant, E. R. Morris, D. A. Rees, P. J. C. Smith, and D. Thom, "Biological interactions between polysaccharides and divalent cations: The egg-box model," *FEBS Letters*, vol. 32, pp. 195-198, 1973.
- [46] G. T. Hermanson, *Bioconjugate Techniques*: Elsevier Science, 2013.
- [47] C. K. Kuo and P. X. Ma, "Ionically crosslinked alginate hydrogels as scaffolds for tissue engineering: Part 1. Structure, gelation rate and mechanical properties," *Biomaterials*, vol. 22, pp. 511-521, 2001.
- [48] J. P. Gong, Y. Katsuyama, T. Kurokawa, and Y. Osada, "Double-Network Hydrogels with Extremely High Mechanical Strength," *Advanced Materials*, vol. 15, pp. 1155-1158, 2003.
- [49] J. P. Gong, "Why are double network hydrogels so tough?," *Soft Matter*, vol. 6, p. 2583, 2010.
- [50] M. T. Khorasani, H. Mirzadeh, and P. G. Sammes, "Laser surface modification of polymers to improve biocompatibility: HEMA grafted PDMS, in vitro assay—III," *Radiation Physics and Chemistry*, vol. 55, pp. 685-689, Aug. 1, 1999.
- [51] P. C. Nicolson and J. Vogt, "Soft contact lens polymers: an evolution," *Biomaterials*, vol. 22, pp. 3273-3283, Dec. 15, 2001.

- [52] H. Zhang, J. K. Jackson, C. Bian, H. M. Burt, and M. Chiao, "Enzyme-Modified Hydrogel Coatings with Self-Cleaning Abilities for Low Fouling PDMS Devices," *Advanced Materials Interfaces*, vol. 2, p. 1500154, 2015.
- [53] G. Skjåk-Bræk, H. Grasdalen, and O. Smidsrød, "Inhomogeneous polysaccharide ionic gels," *Carbohydrate Polymers*, vol. 10, pp. 31-54, 1989.
- [54] B. B. Crow and K. D. Nelson, "Release of bovine serum albumin from a hydrogel-cored biodegradable polymer fiber," *Biopolymers*, vol. 81, pp. 419-27, Apr. 15, 2006.
- [55] H. J. Kong, D. Kaigler, K. Kim, and D. J. Mooney, "Controlling Rigidity and Degradation of Alginate Hydrogels via Molecular Weight Distribution," *Biomacromolecules*, vol. 5, pp. 1720-1727, Sep. 1, 2004.
- [56] O. Smidsrød and G. Skjåk-Bræk, "Alginate as immobilization matrix for cells," *Trends in Biotechnology*, vol. 8, pp. 71-78, 1990.
- [57] X. Zhao, N. Huebsch, D. J. Mooney, and Z. Suo, "Stress-relaxation behavior in gels with ionic and covalent crosslinks," *J Appl Phys*, vol. 107, p. 63509, Mar. 15, 2010.
- [58] L. R. Carr, Y. Zhou, J. E. Krause, H. Xue, and S. Jiang, "Uniform zwitterionic polymer hydrogels with a nonfouling and functionalizable crosslinker using photopolymerization," *Biomaterials*, vol. 32, pp. 6893-9, Oct. 2011.
- [59] L. R. Carr, H. Xue, and S. Jiang, "Functionalizable and nonfouling zwitterionic carboxybetaine hydrogels with a carboxybetaine dimethacrylate crosslinker," *Biomaterials*, vol. 32, pp. 961-8, Feb. 2011.
- [60] W. D. Callister and D. G. Rethwisch, *Materials science and engineering : an introduction*, 2014.
- [61] K. Kabiri, H. Omidian, S. A. Hashemi, and M. J. Zohuriaan-Mehr, "Synthesis of fast-

- swelling superabsorbent hydrogels: effect of crosslinker type and concentration on porosity and absorption rate," *European Polymer Journal*, vol. 39, pp. 1341-1348, Jul. 2003.
- [62] B. Müller, J. Ratia Garcia, F. Marti, and T. Leippold, "MECHANICAL PROPERTIES OF URETHRAL TISSUE," *Journal of Biomechanics*, vol. 41, p. S61, Jul. 7, 2008.
- [63] J. Zhu and R. E. Marchant, "Design properties of hydrogel tissue-engineering scaffolds," *Expert Rev Med Devices*, vol. 8, pp. 607-26, Sep. 2011.
- [64] J. L. Drury and D. J. Mooney, "Hydrogels for tissue engineering: scaffold design variables and applications," *Biomaterials*, vol. 24, pp. 4337-4351, Nov. 2003.
- [65] M. E. Freeman, M. J. Furey, B. J. Love, and J. M. Hampton, "Friction, wear, and lubrication of hydrogels as synthetic articular cartilage," *Wear*, vol. 241, pp. 129-135, Jul. 31, 2000.
- [66] J. A. Rowley, G. Madlambayan, and D. J. Mooney, "Alginate hydrogels as synthetic extracellular matrix materials," *Biomaterials*, vol. 20, pp. 45-53, Jan. 1999.
- [67] C. G. Williams, A. N. Malik, T. K. Kim, P. N. Manson, and J. H. Elisseeff, "Variable cytocompatibility of six cell lines with photoinitiators used for polymerizing hydrogels and cell encapsulation," *Biomaterials*, vol. 26, pp. 1211-8, Apr. 2005.
- [68] A. K. Burkoth, J. Burdick, and K. S. Anseth, "Surface and bulk modifications to photocrosslinked polyanhydrides to control degradation behavior," *J Biomed Mater Res*, vol. 51, pp. 352-9, Sep. 5, 2000.
- [69] N. E. Fedorovich, M. H. Oudshoorn, D. van Geemen, W. E. Hennink, J. Alblas, and W. J. Dhert, "The effect of photopolymerization on stem cells embedded in hydrogels," *Biomaterials*, vol. 30, pp. 344-53, Jan. 2009.
- [70] S. J. Bryant, C. R. Nuttelman, and K. S. Anseth, "Cytocompatibility of UV and visible light photoinitiating systems on cultured NIH/3T3 fibroblasts in vitro," *Journal of Biomaterials*

- Science, Polymer Edition*, vol. 11, pp. 439-457, 2000.
- [71] F. Khademolhosseini and M. Chiao, "Fabrication and Patterning of Magnetic Polymer Micropillar Structures Using a Dry-Nanoparticle Embedding Technique," *Journal of Microelectromechanical Systems*, vol. 22, pp. 131-139, 2013.
- [72] S. Rose, A. Prevoteau, P. Elziere, D. Hourdet, A. Marcellan, and L. Leibler, "Nanoparticle solutions as adhesives for gels and biological tissues," *Nature*, vol. 505, pp. 382-5, Jan. 16, 2014.
- [73] D. Bodas and C. Khan-Malek, "Formation of more stable hydrophilic surfaces of PDMS by plasma and chemical treatments," *Microelectronic Engineering*, vol. 83, pp. 1277-1279, 2006.
- [74] J. P. Gong, "Friction and lubrication of hydrogels—its richness and complexity," *Soft Matter*, vol. 2, pp. 544-552, 2006.
- [75] Y. Murali Mohan, K. Lee, T. Premkumar, and K. E. Geckeler, "Hydrogel networks as nanoreactors: A novel approach to silver nanoparticles for antibacterial applications," *Polymer*, vol. 48, pp. 158-164, 2007.

## **Appendices**

### **Appendix A : Fabrication Process of PDMS-Coated Glass Coverslip**

3 in × 1 in × 1 mm microscope slides were washed with acetone and distilled water. After being dried in air, the slides were cleaned by air plasma (700 mTorr and 30 W) for 75 s. A mixture of PDMS pre-elastomer and curing agent (10:1 weight ratio) was spin-coated onto the slides at 1500 RPM for 60 s, and then the slides were incubated in a 60°C oven for 4 h.

## **Appendix B : Double-Network Alginate-pHEMA Hydrogel Synthesis**

DN hydrogels of various monomer and crosslinker contents were prepared for mechanical property test. Monomer and crosslinker content was fixed in Steps 1 and 2, respectively.

Step 1: SN hydrogel dishes were immersed in 10 vol-% ethyl alcohol solution containing 2 M HEMA, 0.5 wt-% Irgacure 651 and 1 wt-% Irgacure 2959, and various amounts of MBAA (0, 0.5, 1, 2.5, and 4 mol-%) and incubated for 24 h. Then, each side of the gel dish was exposed to 365 nm UV light for 20 min. The resulting DN hydrogel dishes were rinsed with 70% ethyl alcohol and DI water, and then immersed in PBS solution for 36 h prior to the compression test.

Step 2: Separately, SN hydrogel dishes were incubated in 10 vol-% ethyl alcohol solution of various amounts of HEMA monomers (1 M, 2 M and 3 M) containing 0.5 wt-% Irgacure 651, 1 wt-% Irgacure 2959, and 2.5 mol-% MBAA for 24 h. Each side of the gel dish was then exposed to 365 nm UV light for 20 min. After polymerization, the resulting DN gel dishes were rinsed with 70% ethyl alcohol and DI water, and soaked in PBS solution for 36 h.

The weights of both photoinitiators Irgacure 651 and Irgacure 2959 were calculated with respect to the gross weight of the solution, and the crosslinker MBAA concentration in mol-% was calculated with respect to the HEMA monomer content. Because Irgacure 651 does not dissolve in water, and Irgacure 2959 has relatively low aqueous solubility, to fully dissolve these two photoinitiators, they were added to 100% ethanol first in accordance to the amount of HEMA monomers, instead of being added to 10% ethyl alcohol directly. Subsequently, distilled water was added to the mixture to reach the aforementioned concentrations. The resulting pre-gel solution was agitated in a water mixer until no solid was observed.

## **Appendix C : ImageJ Operation Guide**

- 1) Select “file” and “open,” then open the desired image.
- 2) Click “image,” “type” and “16-bit” to convert the image to 16-bit.
- 3) Click “process”, “subtract” and “background” and set “rolling ball radius” to 20 pixels, then tick “light background” and “preview” to subtract image background.
- 4) Select “image,” “adjust” and “threshold” and adjust the bottom bar until the red image best matches the original image, then click “apply” to adjust the threshold.
- 5) Click “analyze” and “measurement” to acquire the percentage confluence measurement.

## **Appendix D : Fabrication procedures for Micropillar Substrate Cast**

The master was made from Asiga PlasWHITE pre-polymer and printed at a resolution of 0.01 mm per layer. Afterward, the part was washed twice with 2-propanol thoroughly and air dried on the bench. It was then post-cured in a Asiga FLASH for 9 min. Then, the master was glued to the bottom of a medium-sized petri dish, and Sylgard 184 silicone (pre-elastomer and curing agent ratio 5:1) was poured into the petri dish to create the negative of the master. After being degassed and cured at room temperature for 48 h, the negative was treated with air plasma for 75 s (700 mTorr and 30 W) and coated with HMDS at room temperature for 24 h. A duplicate of the master was made from Sylgard 184 silicone (pre-elastomer and curing agent ratio 10:1) and cast in the negative and cured at room temperature for 48 h after the degassing process. Finally, thoroughly mixed Smooth-Cast 310 (Smooth-On, Inc., PA, USA) was poured onto the duplicate and left overnight at room temperature to create the plastic mold. To eliminate air bubbles in the plastic mold, the cured PDMS duplicate was degassed for at least 30 min prior to the last step.

## Appendix E : Ribbon Design for Hydrogel Adhesion Strength Test

The master contained three test strips; each had a  $1\text{ cm} \times 1\text{ cm}$  square area covered in micropillars. The height and diameter of each micropillar was  $200\text{ }\mu\text{m}$  and  $150\text{ }\mu\text{m}$ , respectively. The distance between micropillars was  $350\text{ }\mu\text{m}$ .

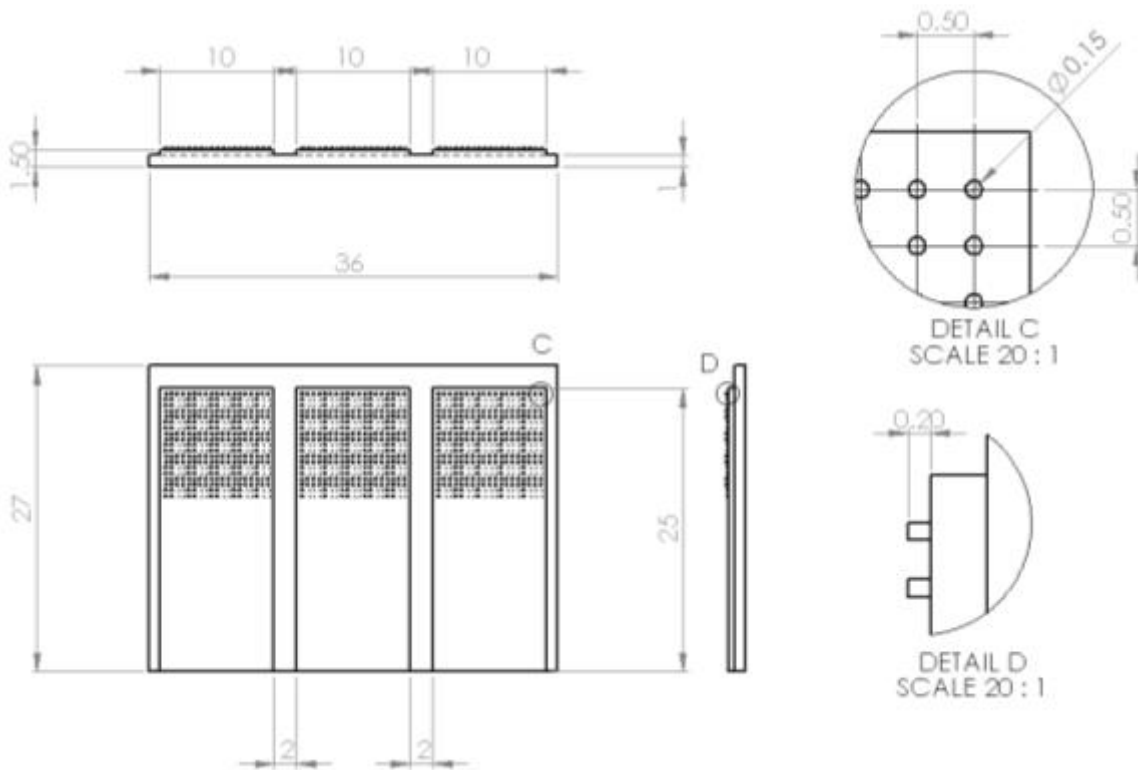


Figure A.1 The schematics of the master